INVESTIGATION OF THE BIOLOGICAL HEALTH POTENCY OF FIG STALK WASTE PECTIN FOR COLON CANCER CELL GROWTH AND INTESTINAL GLUCOSE ABSORPTION

A Thesis Submitted to
the Graduate School of Engineering and Sciences of
İzmir Institute of Technology
in Partial Fulfillment of the Requirements for the Degree of

MASTER OF SCIENCE

in Food Engineering

by
Filiz BAŞER

July 2022
İZMİR

ACKNOWLEDGEMENTS

It is a pleasure to acknowledge my deepest gratitude and appreciation to Assoc. Prof. Dr. Şükrü GÜLEÇ for his supervision and guidance regarding research in his laboratory. This thesis is constructed with his valuable advice and persistent help. I have been supported by him to do independent research and encouraged to stick to doing science. It is an honor to complete my master's thesis studies at Güleç Laboratory. I would like to extend my gratitude to my co-advisor Prof. Dr. Ahmet YEMENİCİOĞLU for his support, guidance, and critical recommendations in this research.

I would like to thank current members of Güleç Laboratory, Cansu ÖZEL TAŞÇI, Ayşegül ALYAMAÇ, Eda DALYAN, Bengisan DİVRİK, and former member Dr. Ezgi EVCAN for their kind assistance with experimental approaches and contributions.

I owe special thanks to Elif & Çağrı ÇAVDAROĞLU for their motivations, friendship, and valuable contributions during my master's studies.

I would like to express my deep sense of thanks and gratitude to my dear friend, Anıl Can ÖNDER. He always stands by me to weather the storm.

I would like to acknowledge the Scientific and Technological Research Council of Turkey (TUBITAK) for supporting this project (118O372) financially.

I reserved the end of acknowledgment to my wonderful parents, Nezihan & Hamit BAŞER for their endless love, support, and kindness. Also, I am grateful to my sisters Ceyda & Emine Eda, and my brother Mustafa for their love and emotional support.

ABSTRACT

INVESTIGATION OF THE BIOLOGICAL HEALTH POTENCY OF FIG STALK WASTE PECTIN FOR COLON CANCER CELL GROWTH AND INTESTINAL GLUCOSE ABSORPTION

Higher intake of dietary fiber is correlated with reduced obesity-related disorders such as cardiovascular diseases and diabetes, improved gut health, and protection against colorectal cancer. Pectin comes from plant cell walls and is mainly composed of galacturonic acid units branched with neutral sugars that provide bioactive and functional properties. Pectin has long been appreciated in the food industry due to its viscous structure and gelling properties. Dietary pectin as a soluble fiber is linked with cancer and metabolic health. Anti-cancer activity of pectin is promising in multiple types of cancer in humans and animals by inducing cellular apoptosis and inhibiting tumor metastasis. Soluble dietary pectin regulates blood glucose levels, sparking interest in diabetes prevention and treatment. Fig stalk waste was used as an unconventional pectin source in the present study, providing a promising green option. The health benefit of fig stalk waste pectin (FSWP) was investigated in terms of colon cancer cell growth and intestinal glucose absorption. The inhibitory effects of FSWP on colon cancer Caco-2 cells were further confirmed with cell cycle analysis and apoptotic cell death. Intestinal glucose absorption was modeled with Caco-2 enterocyte uptake and transport systems. FSWP inhibited 2-deoxyglucose uptake into Caco-2 cells and reduced glucose absorption as a food ingredient in the intestinal transport system. Taken together, FSWP has promising bioactivity against colon cancer and could be used as a functional food additive due to its inhibitory effect on intestinal glucose absorption.

ÖZET

İNCİR SAP ATIĞI PEKTİNİNİN KOLON KANSER HÜCRE BÜYÜMESİ VE İNCE BAĞIRSAK GLİKOZ EMİLİMİ İÇİN BİYOLOJİK SAĞLIK POTANSİYELİNİN İNCELENMESİ

Diyet lif içeriği yüksek gıdalar kardiyovasküler hastalıklar ve diyabet gibi obeziteye bağlı gelişen metabolik hastalıkların önlenmesi, bağırsak sağlığına ve kolon kanserine koruyucu etkileriyle bilinmektedirler. Pektin lifi bitkilerin hücre duvarlarında yapı maddesi olarak görev alan biyoaktif ve fonksiyonel özellikler taşıyan bir moleküldür. Pektin viskoz yapısı ve jelleştirme etkisi ile gıda sektöründe uzun yıllardır aktif bir şekilde kullanılmaktadır. Biyomedikal, ilaç ve kozmetik sektörlerinde de teknolojik fonksiyonel özellikleri ve sağlık üzerindeki olumlu etkileri nedeniyle kullanılmaktadır. Çözünebilir pektin kanserden koruma etkisi ve metabolizma üzerindeki olumlu etkileri ile dikkat çekmiştir. Birçok farklı dokuda kansere karşı koruyucu aktivite gösteren pektin apoptoz ile kanser hücre ölümünü destekleyip tümör metastazını engelleyebilmiştir. Aynı zamanda diyetten gelen pektinin kandaki glikoz seviyesini düşürdüğü gözlemlenmiş ve glikoz metabolizmasının regülasyonuna bağlı diyabete karşı koruma veya tedaviye yönelik ilgiyi üzerine çekmiştir. Bu çalışmada incir sap atığından elde edilen pektinin kolon kanser hücre büyümesine ve glikoz emilimine etkisi araştırılmıştır. Tezin ilk kısmında incir sap atığı pektininin Caco-2 kolon kanser hücrelerinin büyümesini engellemeye yönelik etkisi hücre döngüsü ve apoptotik hücre ölümü analizi ile araştırılmıştır. Bağırsakta glikoz emilimi hücresel alım ve geçiş sistemleri olarak Caco-2 enterosit hücreleri kullanılarak modellenmiştir. İncir sap atığı pektini 2-deoksiglikoz alımını düşürürken bağırsak geçiş sisteminde glikoz geçişini azaltıcı yönde etki ettiği gözlemlenmiştir. Bağırsak geçiş sisteminde incir sap atığı pektini yoğurda eklenerek fonksiyonel gıda geliştirilmesi için uygulanabilirliği ortaya konulmuştur. Hepsi birden değerlendirildiğinde incir sap atığı pektini kolon kanser hücrelerine karşı biyoaktivite göstermiş ve fonksiyonel gıda katkısı olma potansiyeli glikoz emilimi azaltması ile ortaya konulmuştur.

TABLE OF CONTENTS

LIST OF FIGURES

Figure **Page**

LIST OF TABLE

Table **Page**

CHAPTER 1

INTRODUCTION

The first chapter of the thesis covers a general overview of dietary fibers and their influence on metabolic health and diseases. Then, it focuses on pectin as a dietary fiber, the structure and composition of pectin, and the functional applications of pectin in a variety of fields. It follows by reviewing the health benefits of pectin and its bioactive potential for human health. It then discusses the possibility of fig as a source of pectin and examines the applicability of fig stalk waste pectin (FSWP) to improve food's health benefits and nutritional value**.**

1.1. Dietary fiber

Dietary fiber is edible plant matter, resistant to human digestion and absorption in the small intestine. Some of the dietary fibers can be digested by GI tract bacteria. Dietary fibers include non-starch polysaccharides such as cellulose, hemicellulose, heteropolymers (pectin), β-glucans, polyfructoses, natural gums, and mucilage; non-polysaccharides such as lignin. They differ depending on their structural, physical, and chemical characteristics, namely water solubility, viscosity, fermentability, and binding-bulking ability (J. Slavin, 2013). Dietary fiber is listed on the Nutrition Facts labels on food products. Nutritional guidelines recommend 25 g of dietary fiber daily for adult women and 38 g for adult men (J. L. Slavin, 2008).

1.1.2. Effects of dietary fibers on metabolic health

Dietary fiber intake has a beneficial impact on preventing developing chronic diseases. Dietary fibers have been linked with improved glucose homeostasis and reduced risk of developing metabolic conditions such as obesity and type-2 diabetes mellitus (T2D). These effects correspond with the regulation of gastric emptying rate and the

transit of food in the small intestine and colon. Separating dietary fibers into their fractions and concentrating those components in a diet has become a perspective to determine their impact on health. Soluble dietary fibers (SDF) generate a dense structure and form a gel when dissolving in water. This physicochemical characteristic of SDF is correlated with its impact on intestinal motility and glucose, cholesterol, and triglycerides absorption rates.

1.2. Pectin as a soluble fiber and gut metabolism

Dietary fibers directly interact with the immune barrier in the small intestine. The mucus layer facilitates the interaction of dietary molecules with intestinal epithelial and immune cells.

1.2.1. Pectin structure and composition

Pectin structure is generally modeled as the main backbone of homogalacturonan (HG), intercalating with rhamnogalacturonan-I (RG-I) and rhamnogalacturonan-II (RG-II) polysaccharides in a chain-like configuration (Figure 1.1). Backbone structure branches with other neutral sugar chains such as xylogalacturonan (XGA), arabinogalactan I (AG-I), and arabinogalactan II (AG-II). It varies in length between 100-1000 saccharide units. Pectin structure comprises 65% HG region, 20-35% RG-I and other substituted galacturonans in the remaining portion. HGs are made up of D-galacturonic acid (GalA) units bound one to the other through α-(1→4) glycosidic linkages presenting the smooth regions of the pectin polymer. GalA residues, depending on the source, constitute 72-100% of the HG backbone structure. For instance, the HG backbone of citrus pectin contains 80-95% GalA residues. Furthermore, the carboxyl group of some GalA residues can be methyl esterified at C-6 and/or o-acetylated at C-2 and C-3. HG backbone is susceptible to enzymatic and mechanical de-esterification and degradation.

RG-I polysaccharide is formed by repeating units of α-(1→2) linked rhamnose and α-(1→4) linked GalA residues that can be o-acetylated at O-2 and/or O-3 positions. It is a highly branched and heterogeneous polysaccharide substituted by galactans and

arabinans at the O-4 position. Also, polymeric side chains of AG-I and AG-II could be referred to as hairs. The solubility of pectin has been correlated with the hairy side chains (Naqash et al. 2017a). RG-II is composed of approximately 9 GalA residues backbone. There are bound monosaccharides onto the backbone such as apiose, acetic acid, 3-deoxy-manno-2-octulosonic acid (KDO), and 3-deoxy-xo-2-heptulosaric acid (DHA) as side chains(Voragen et al. 2009). RG-II backbone may be methyl-esterified at the C-6 position of GalA residues. The percentage of esterified GalA and acetylated groups in the HG backbone are the degree of esterification (DE) and degree of acetylation (DA), respectively. In the early stages of plant development, pectin is highly esterified, and de-esterification occurs through the development of the cell wall. DE differs in the 60-95% range in plant tissue pectin. The extraction method and origin of the plant affect the variation of DE and DA, which eventually determine the functionality of pectin. Depending on DE, pectin is classified as high methoxy pectin (HMP) and low methoxy pectin (LMP). HMP varies between 60-75 % DE whereas LMP varies from 20-40 % DE. Structural features such as viscosity, solubility, and gelation properties significantly impact functional characteristics.

Pectin is a structural heteropolysaccharide that gives mechanical solidity to plants and provides a barrier to the external environment(Taboada, Fisher, Jara, Zúñiga, et al. 2010). HGs and RGII provide cell wall rigidification. HGs form the structures called egg boxes by binding chain to chain to each other. Bivalent Ca^{+2} ions intercalate between two HG chains which is the process important for the gelling property of pectin. RG-I plays a role in cell plasticity by preventing HG chain interaction with Ca^{+2} ions. Pectin organization and composition in plant primary cell walls vary depending on the growth state of the plant, localization within the plant, and the plant origin.

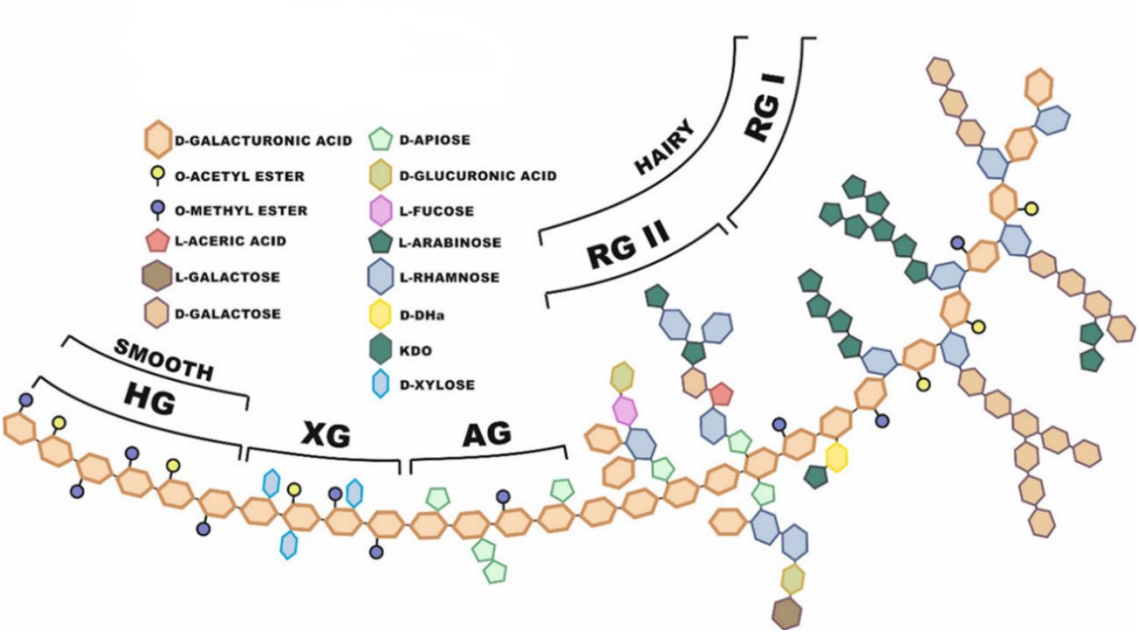

Figure 1.1. Pectin structure schema. Demonstrating the homogalacturonan (HG), xylogalacturonan (XG), apiogalacturonan (AG), rhamnogalacturonan II (RG-II), and rhamnogalacturonan I (RG-I) regions.The smooth, partially esterified HG backbone constituting the linear region is the dominating structure representing up to 60% of the total pectin. The hairy areas cover highly branched RG I and RG II domains and XG and AG at a lesser extent (Zdunek et al., 2021).

1.2.2. Pectin applications and functional properties

Pectin is a natural hydrocolloid valued in various functional applications such in the food, cosmetic and pharmaceutical industries. It is possible to extract pectin and enrich its functionality. In addition to the developmental stages of plants and origin, the extraction method affects the pectin composition and structure. Thus, there are various functional properties of pectin, including emulsifier, gelling agent, thickener, stabilizer, fat or sugar replacer in low-calorie foods, and being an active ingredient in foods. Pectin can improve viscosity or thickness due to its water-binding and gel-forming properties even at low concentrations. Therefore, it is widely used in the food industry as a gelling agent and thickeners such as jams, bakery fillings, and confectionery. Another wide application of pectin in food is as a stabilizer in yogurts and milk drinks. It is also used to

give firmness to ice cream, salad dressings, gravy, and many other food products. In addition, utilized pectin from different sources has been modeled as a fat replacer in various food systems such as cheeses (Lobato-Calleros et al. 1999; 2001), low-fat frankfurters (Candogan and Kolsarici 2003; Pappa, Bloukas, and Arvanitoyannis 2000) and cookies (Min et al. 2010). Other relevant applications of pectin are personal care products (toothpaste, shampoos, and paints), pharmaceuticals (gel caps), and cosmetics.

1.2.3. Modified pectin and other trend applications in health

Native pectin can be broken down into smaller fragments to improve its functionality and bioactivity. Certain modifications can enable pectin for various applications in biomedicine, drugs, agriculture, and food. Production of edible coatings and antimicrobial bio-based films to protect foodstuff are some trends in the food industry. Also, modified pectin can be used in producing nanoparticles, healing agents, and cancer treatment. Technologies enabling to reveal of structure/function relationships of pectin at the molecular level allow designing pectin with specific desired functionalities. For instance, pectin as an encapsulating agent is a trend in drug delivery systems that promotes controlled release and helps avoid drug degradation (Martău, Mihai, and Vodnar 2019). Modified citrus pectin (MCP) obtained by high pH and temperature has emerged as a promising anti-metastatic drug. MCP shows potent inhibition of melanoma and prostate carcinoma. Modifying pectin by chemical, enzymatic and physical treatments empowers the bioactivity and possesses greater antitumor action than its native form (Naqash et al. 2017b). Citrus pectin modified by temperature exhibits apoptotic activity in human prostate cancer cells (Jackson et al. 2007).

1.3. Potential Applications of Pectin in the Health and Biomedical Industry

In 2010, the European Food Safety Authority (EFSA) published scientific opinions on nutrition and pectin's health claims (EFSA Panel on Dietetic Products 2010). They recognized the validity of scientific data on reducing post-prandial glycemic

responses, maintaining blood cholesterol levels (Brown et al., 1999), and reducing energy intake by increasing satiety (di Lorenzo et al. 1988). Recognition of pectin leads to an increased usage of pectin as a health ingredient and nutritional supplement. Health claims of pectin have been raised due to its effects on metabolic and chronic diseases.

1.3.1. Pectin effects on serum glucose and cholesterol-lowering ability

Pectin displays a gelling property in the digestive tract, slows digestion, and prolongs gastric emptying. Dumping syndrome patients with too rapid digestion benefit from pectin consumption (Lawaetz et al. 1983). While increasing nutrient transit time, the viscosity of the digestive tract is also increased, leading to prolonged satiety, controlled energy intake, and weight management. SDF, including pectin, slows down the digestion of macronutrients and delay gastric emptying, leading to slow transport and mixing of digestive enzymes. Also, it increases the thickness of the unstirred water layer at the intestinal mucosa, which causes a reduction in intestinal motility. Consequently, these combined effects decrease the intestinal absorption of glucose, fatty acids, and cholesterol. The lower rate of glucose absorption leads to a decline in insulin levels. Type-2 diabetic rats administered with citrus pectin showed a reduction in fasting blood glucose levels and improvement in insulin resistance after four weeks of treatment. In addition, it improved hepatic glycogen content and blood lipid levels (Liu et al. 2016). Diets rich in pectin are correlated with enhancing bile acid excretion and consequently reducing cholesterol levels, following a favorable impact in lowering heart diseases (Brouns et al. 2012). Pectin in high- and low-fat diets leads to a reduction in the levels of leptin, insulin, total cholesterol, and triglycerides in rats (Adam et al. 2015). This cholesterol-lowering impact of SDF has been explained with three different mechanisms of action. Usually, excess bile acid can be reabsorbed into the system by the small intestine and transported back to the liver as a feedback mechanism. The first possible mechanism is that SDF might hinder bile acid reabsorption into the enterohepatic circulation due to high viscosity (Brouns et al. 2012). Another possibility is that SDF triggered a reduction in glucose absorption, leading to a decline in insulin production in the pancreas. Insulin activates HMG-Co A reductase enzyme, a rate-controlling enzyme in hepatic cholesterol synthesis. Consequently, reduced insulin levels result in a reduced rate of cholesterol synthesis. Highly viscous SDF may alter small micelles' formation and trigger overall cholesterol

absorption reduction. Also, fermentation of fiber by gut microbiota and SCFA production may change hepatic cholesterol production. Propionate depletes blood cholesterol levels by inhibiting cholesterol biosynthesis in the liver (Gunness and Gidley 2010). The cholesterol-lowering ability of pectin is associated with DE, viscosity, molecular weight, and the presence of acetylation or amidation. Pectin forms a viscous gel, binds to cholesterol and bile acids, promotes excretion of bile acids, and reduces its reabsorption. Highly viscous lemon peel pectin had a more significant reduction in blood and liver cholesterol and more fecal excretion of sterol than low viscous lemon peel pectin in hamsters (Terpstra et al., 2002). Also, research indicates that high molecular weight pectin lowers cholesterol levels more effectively than low molecular weight pectin (Wicker et al. 2014). Espinal-Ruiz et al. (2016) demonstrated lipid digestion under-stimulated gastrointestinal conditions to show the impact of pectin nature on lipid digestion profile(Espinal-Ruiz et al. 2016). Increased molecular weight and methoxylation diminished the extent of lipid digestion. Pectin with a higher methoxylation degree changed the rheological properties of gastrointestinal fluids by increasing hydrophobicity (Figure 1.2). Therefore, pectin promotes metabolic health by lowering glycemic response and cholesterol levels due to its physicochemical properties.

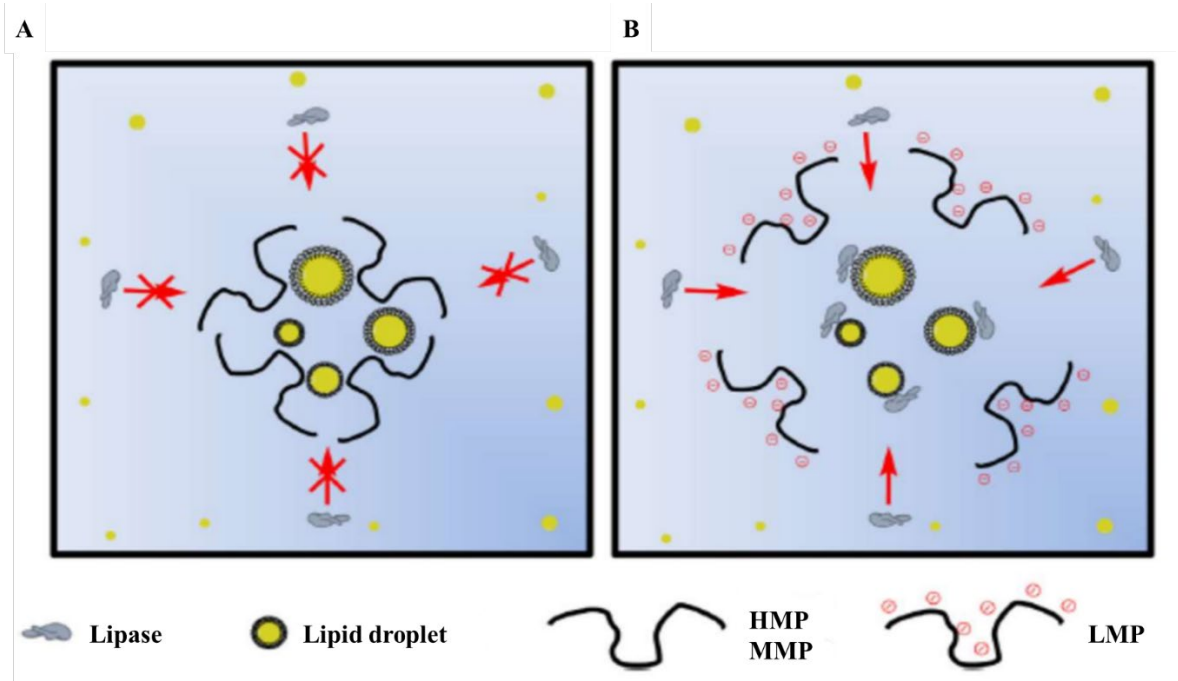

Figure 1.2. The illustration shows pectin behavior to inhibit lipid droplet digestion; (A) High and medium methoxyl pectin; (B) Low methoxyl pectin (Lara-Espinoza et al. 2018)

1.3.2. Anti-cancer activities of pectin

Using natural compounds to develop new therapies is a target in cancer-related research. Bioactive components that can induce apoptosis and inhibit cancer cell growth arouse interest as dietary pectin. Pectin has a heterogeneous structure which provides a variety in functionality and bioactivity. Delphi and Sepehri (2016) showed that apple pectin triggered antitumor activity in 4T1 breast cancer cells. In addition, tumor progression is inhibited, and apoptosis is increased *in vivo* by apple pectin (Delphi and Sepehri 2016). Ginseng pectin and its fractions were analyzed for cancer cell growth and showed growth inhibition and cell cycle arrest in the G2/M phase in colon cancer HT-29 cell line (Cheng et al. 2011). Small molecular weight pectin fractions usually rich in arabinose and galactans can interact with the carbohydrate recognition domain (CRD) on galectin-3 (GAL3) protein. GAL3 is a pro-metastatic protein that promotes cell adhesion and migration and prevents apoptosis. Swallow root pectin polysaccharides and citrus pectin shows high GAL3 inhibitory activity. On the other hand, ginger-derived pectic polysaccharides did not inhibit GAL3, which might be correlated with low galactose levels. Evidence also suggests that the alignment of galactose and arabinose as arabinogalactan significantly impacts the inhibition of GAL3. Therefore, pectin's structure/bioactivity relationship is very complex, causing a large variety in functionality. CRD-mediated interaction of GAL3 provides cell-cell contact and connection with the extracellular matrix, which regulates cell aggregation, chemotaxis, and angiogenesis. Additionally, GAL3 locates inside the cell and plays an intracellular role in regulating apoptosis and maintaining tissue homeostasis. Anti-apoptotic BCL-2 protein found on the mitochondrial membrane is one of the ligands of GAL3. GAL-3 binds to BCL-2, which activates BAX protein downstream to prevent apoptosis. Optimizing a GAL3 inhibitor might be utilized as a non-toxic strategy to avoid or reduce carcinogenesis.

Another possible interaction of pectin to explain anticancer activity is through an immune response. Cyclooxygenase-2 (COX-2) and inducible nitric oxide synthase (iNOS) are expressed after LPS treatment to macrophages. COX-2 and prostaglandins are associated with cancer development in multiple epithelial tissues. NO level is contributed to several conditions such as inflammation and cancer. Chen et al. (2006) reveal that citrus pectin is inhibited COX-2 and NOS expression levels in LPS-activated macrophages (Chen et al. 2006). Another study reported that sweet pepper pectin increased the

secretion of cytokines such as IL-1, IL-10, and TNF-α by THP-I macrophages (do Nascimento et al., 2017). Immunomodulatory activity is also observed in *Ficus carica* polysaccharides that enhance phagocytosis, activate cytokine production in mouse macrophages, immune response, and promote probiotics growth (Du et al. 2018a). Dietary pectin exhibits anti-tumor activities because it inhibits tumor growth and regulates oncogenes.

1.3.3. Removal of metal ions

Pectin has also been investigated for its potential to promote ^{137}Cs clearance. ^{137}Cs, radio-isotope of cesium was produced during uranium fission in Chernobyl area caused children to have cesium loads. Apple pectin was given to children who have moderate and high cesium loads as a food additive for 16 days. They showed a significant reduction at ^{137}Cs levels, showing pectin's ability to increase the cleansing of heavy metals (Bandazhevskaya et al., 2004). Also, pectasol addition to the diet has improved the intoxication of arsenic and cadmium through elimination by urinary track (Eliaz et al., 2006).

1.3.4. Prebiotic effect

Pectin can be metabolized by gut microbiota favoring colonic bacteria to increase in number. Specific pectin fractions depending on prebiotic index and composition, promote the growth of *Bifidobacterium* and *Lactobacillus* species known for improving digestion and decreasing inflammation. Good bacteria produce short-chain fatty acids (SCFAs) such as butyrate, acetate, and propionate. *In vivo* studies reveal that SCFAs trigger cytokine production to support the immune system (D'Souza et al. 2017). Also, SCFAs control cellular growth in cancer (Park et al. 2019).

1.4. Fig as a source of pectin

Ficus carica fig tree cultivation originated in Central Asia and the Mediterranean coast in ancient times. Fig fruit can be processed into wine, jam, or fruit juices and has

been recognized as medicine and food for centuries. Fig plant has been reported to improve appetite, treat diarrhea, and be used as a gargle for sore throat. Figs are rich in phenolic compounds and flavonoids, which exhibit biological activities. Also, natural polysaccharides from figs have been recognized as bioactive compounds with biological health potency. A novel polysaccharide extracted from *Ficus carica* showed an immune-modulatory effect by activating macrophage cells *in vitro* (Du et al. 2018b). There are studies on the health effects of pectin from *Ficus carica*. Antitumor activity of pectin from fig skin was investigated on HepG2, and A549 cancer cell lines and an inhibitory effect on cell proliferation was reported *in vitro* (Gharibzahedi, Smith, and Guo 2019).

The Sun-drying process is an ancient method for fruits that are highly affected by the climate and field practices. Therefore, figs are also sensitive in that sense, creating products of various quality. Turkey produces and supplies a large proportion of sun-dried figs in the world. Sun-dried figs are known for their fiber-rich content, especially soluble pectin. When sun-dried figs are processed and packed in shelf-stable forms, stalks are one of the by-products that remain after processing. The project, 118O372, aimed to valorize and investigate the potential of stalk wastes as a source of pectin and form value-added products. For this purpose, they have extracted pectin from waste sun-dried fig stalk and characterized it in terms of functional and molecular properties such as moisture content, carbohydrate content, degree of esterification, and galacturonic acid content. FSWP is extracted with the hot acid method. GA content is detected as 63% (Table 1) using meta-hydroxybiphenol spectrophotometric method using D-galacturonic acid as standard. FSWP has a 68% degree of esterification determined with HPLC analysis that can be classified as high methoxy pectin. Other functional properties such as sugar content, protein content, moisture content, L-rhamnose, L-arabinose, D-glucose, and D-galactose levels of FSWP are listed in table-1.

Table 1. Different characteristics of sun-dried fig stalk waste pectin (FSWP).

Characteristics	SP[a,b]
GA	63.32 ± 6.05
DE	68.33 ± 4.86
Total carbohydrate	89.39 ± 7.06
Moisture content	5.09 ± 0.15
Ash	3.92 ± 0.14
Protein	1.60 ± 0.14
D-Glc	0.80 ± 0.002
L-Rha	1.56 ± 0.30
D-Gal	6.51 ± 0.40
L-Ara	5.12 ± 0.03
R-1	4.09
R-2	0.029
R-3	7.51
R-4	3.86
HG	77.16
RG-I	21.76
HG:RG-I	3.55

[a] Values are shown as mean ± standard deviation.

[b] All values are expressed as % on a dry basis of pectin powder except moisture content.

1.5. Aim of this thesis

In the scope of this thesis, pectin polysaccharide extracted from fig stalk wastes is analyzed in terms of health benefits. The biological activity of FSWP is investigated in two sections. In the first section, the effect of FSWP on colon cancer cell growth is aimed to be acquired by determining cellular toxicity and anticarcinogenic activity on the Caco-2 cell line. Cell cycle distribution and apoptosis-inducing ability of FSWP are analyzed at cytotoxic concentrations. Therefore, the mechanism behind cellular cytotoxicity of FSWP is examined at the molecular level on Caco-2 colon cancer cells. In the second section, the effect of FSWP on glucose uptake and absorption is investigated in the

intestinal uptake and transport system. Intestinal glucose uptake is demonstrated by using glucose analog, and the effect of FSWP on glucose entry is analyzed in terms of intracellular glucose. Furthermore, FSWP is added into yogurt to demonstrate its potential as a functional ingredient. Glucose absorption is detected in the intestinal transport system, and the FSWP effect on glucose efflux is determined. Therefore, FSWP biological activity is examined on glucose uptake and absorption in intestinal enterocyte cells.

CHAPTER 2

METHODOLOGY

The second chapter explains the methodology that is followed in this thesis. Firstly, it explains how the human intestine's modeling works by Caco-2 cell culturing and how it is maintained properly. Also, how the intestinal transport system is formed due to Caco-2 polarization and how it is controlled with transepithelial resistance measurement. Then, the cytotoxicity of FSWP is determined by quantifying Caco-2 cellular viability with WST-8 cell counting kit. Cytotoxic concentrations are used to treat Caco-2 cells to investigate the mechanism behind the reduction in cellular viability. The Caco-2 populations after FSWP treatments are distinguished by cell cycle analysis with PI staining and flow cytometry. Also, the populations are examined regarding triggered apoptosis with Annexin V/PI staining. Following the anticarcinogenic activity, FSWP is examined in terms of intestinal glucose metabolism. FSWP effect on glucose uptake is mimicked by using 2-deoxyglucose on the Caco-2 intestinal uptake system with glucose uptake colorimetric assay. Later, the potential of FSWP as a functional ingredient is demonstrated by addition to yogurt, and the samples are digested to mimic human digestion. Glucose absorption in functional yogurt is shown by using the Caco-2 intestinal transport system, and time-dependent glucose levels are detected by using an enzymatic glucose assay. Therefore, the biological health potency of FSWP is evaluated in terms of colon cancer cell growth and intestinal glucose uptake and absorption.

2.1. Modeling human intestine *in vitro*

The intestinal epithelial barrier has been widely modeled with the human intestinal epithelial cell line, Caco-2. The human colorectal adenocarcinoma epithelial cell line is derived from colon carcinoma, Caco-2 epithelial cells grown as an adherent monolayer in culture. Cells acquire the characteristics of brush-border microvilli at the apical side towards confluency. Adjacent cells polarize and form tight junctions. Caco-2

shows enzyme activities similar to absorptive enterocyte cells. They express digestive enzymes, membrane peptidases, and disaccharidases such as lactase and aminopeptidase N. Also, they actively transport amino acids, sugars, vitamins, and hormones (Lea 2015). Membrane ionic transport through Na^+/K^+ ATPase, H^+/K^+ ATPase, Na^+/H^+ exchange, $Na^+/K^+/Cl^-$ cotransport and apical Cl^- channels are present. Whereas non-ionic transport is valid with permeability glycoprotein, multidrug resistance-associated protein, and lung cancer-associated resistance proteins. In addition to transporters, Caco-2 cells have receptors such as vitamin B12, vitamin D3, EGFR (epidermal growth factor receptor), and sugar transporters (GLUT1, GLUT2, GLUT3, GLUT5, SGLT1). Also, Caco-2 produces cytokines like IL-6, IL-8, TNFα, TGF-β1, TSLP and IL-15. These features and mechanisms ensure that Caco-2 is a valid candidate to model the intestinal epithelial barrier for investigating the uptake, metabolism, and transport of dietary components. Caco-2 cells can be grown on the plastic surface of wells to study apical uptake and metabolism of bio-accessible dietary compounds (Figure 2.1A). Cells can also be grown and differentiated on semi-permeable membranes in inserts placed in wells to create a three-compartment model to investigate dietary compounds' absorption, metabolism and trans-epithelial transport (Figure 2.1B). Also, the transport system can be used to study the effects of compounds, extracts, and digested foods on enterocyte-like cellular functions.

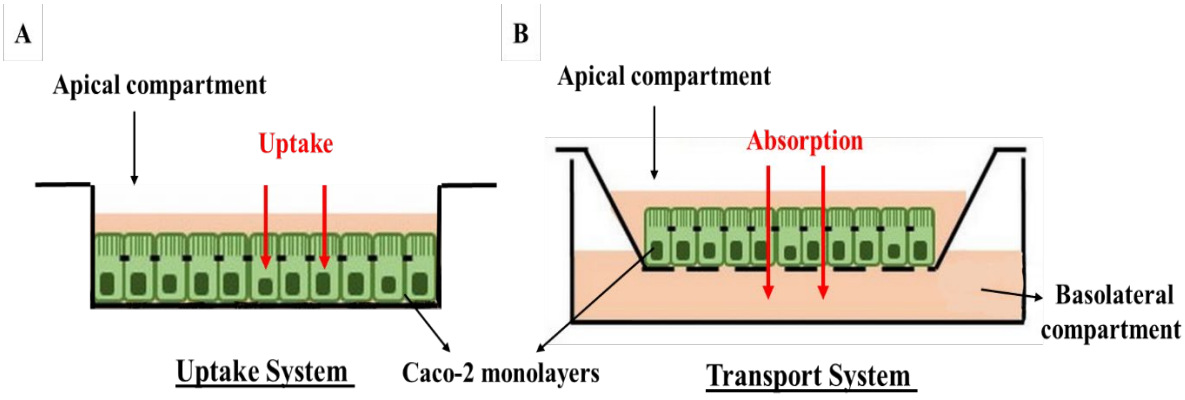

Figure 2.1. Caco-2 cell models; (A) Uptake system; (B) Transport system

2.1.1. General Maintenance

Caco-2 (HTB-37) was purchased from American Type Culture Collection (ATCC). Caco-2 cells were grown in MEM (Sigma, M4655) supplemented with 10% fetal bovine serum (Hyclone, SV30160.03) and the following additions: 1% nonessential amino acids mix (Multicell, 321-011-EL), 1% sodium pyruvates (Capricorn, NPY-B), 1% penicillin and streptomycin solution (Capricorn, PS-B). Caco-2 cells were maintained at 37 °C in a humidified 5% CO_2 atmosphere. Cells reaching 80% confluency were split 1:5 ratio before further cultivation. Cells were rinsed with PBS twice, and 2 ml trypsin/EDTA was added into a 75 cm^2 maintaining flask. The cells were incubated at 37 °C for 2-5 minutes. After detachment, cells were collected with 8 ml maintaining medium, and 2 ml of collected cells were transferred into a new 75 cm^2 flask. The medium was replaced every three days. Generally, it takes 4-5 days for Caco-2 cells to reach 80% confluency. Cells were used between 25-35 passages for further experiments and regularly tested for mycoplasma contamination.

2.1.2. Polarizing Caco-2 cells in tissue culture inserts

Caco-2 cells were grown on permeable filter inserts to generate a polarized human intestinal epithelial barrier. Cultivation on inserts improves Caco-2 cells' functional and morphological differentiation. Polyethylene terephthalate was used for cultivation which allows for following the differentiation process under the inverted microscope with its transparency. The pore size of the filters was 0.4 μm for cellular transport and permeability experiments. 12 mm filter inserts were placed onto 12 well plates, and cells were seeded as $5*10^5$ cells per insert density. The apical compartment in a 12-well insert takes 0.5 ml medium, while the basolateral chamber takes 1.5 ml. Generally, after 3-4 days, cells cover the insert membrane while the process is observed under the microscope. After that, the medium was replaced on both apical and basolateral sides of the membrane every two days. Caco-2 cell monolayers were homogenously differentiated after 18 to 21 days (Figure 2.2).

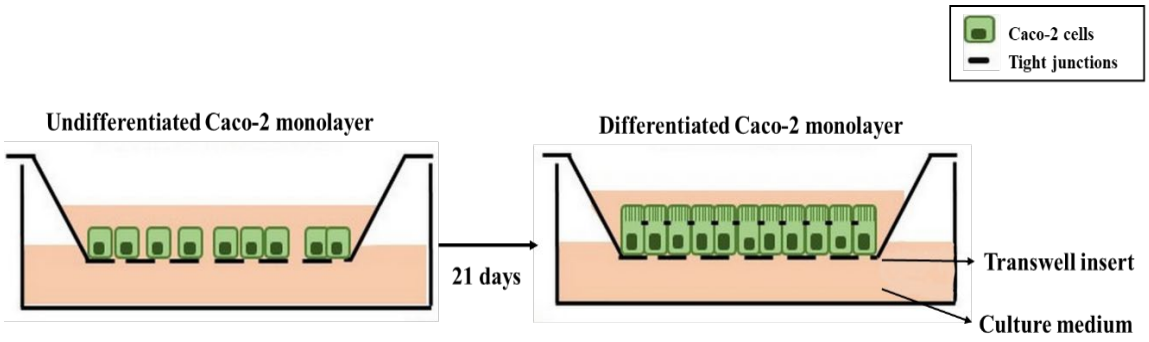

Figure 2.2. Polarizing Caco-2 cells to form a transport system

2.1.3. Transepithelial electrical resistance (TEER) measurement

Barrier function and monolayer integrity are critical parameters to control Caco-2 cell monolayer systems before cellular transport, interaction, and uptake experiments. The protocol based on transepithelial electrical resistance (TEER) is essential to confirm the integrity and quality of polarized epithelial cell monolayer. TEER value was measured with a portable voltmeter, EVOM device (WPI, USA) on 21 days of post confluency (Figure 2.3B). The short electrode was placed into the medium in the upper chamber, while the long electrode was placed into the medium in the lower chamber (Figure 2.3A). The resistance was measured directly with the EVOM device as ohm per cm^2 of the filter insert. Caco-2 cells have high electrical resistance. TEER is stated as at least 250 ohm/cm^2 for Caco-2 cells, and it needs to be reached to proceed with the experiment. 12-well insert wells are used in the transport experiments (Figure 2.3C).

Figure 2.3. Transepithelial Electrical Resistance (TEER) Measurement; (A) TEER is measured by replacing the short electrode in the medium in the upper chamber while the long electrode is placed into the medium in the lower chamber. (B) EVOM device. (C) 12-well insert wells.

2.2. Preparation of FSWP solution for cell culture experiments

FSWP stock solution was prepared as 30 mg/ml (3%) by dissolving in a serum-free medium. FSWP was left on the shaker at room temperature overnight for proper dissolution. The pH of FSWP stock was brought to 7.0 from 4.15. Stock FSWP was diluted in a serum-free medium for further experiments.

2.3. Anticarcinogenic activity of FSWP

Cell proliferation assay was performed to analyze the cytotoxic impact of FSWP on the Caco-2 cell line. Cells were seeded in 96 well plates at a density of 4000 cells/well containing 250 µl culture medium in each well. They were incubated at 37 ºC with 5% CO_2 for 24 hours to adhere. After, the cells were synchronized with a 1% FBS containing medium with overnight incubation. Later, plates were treated with 100 µl of pectin solutions at 50-3000 µg/ml concentration for 72 hours of incubation. Cells were observed under the microscope during the treatment, and images were collected at 72 hours. Cellular viability was quantified with a WST cell counting kit (Sigma-Aldrich, Cell Counting Kit-8). The working principle of the assay is based on the metabolic activity of the cells by WST-8 (2-(2-methoxy-4-nitrophenyl)-3-(4-nitrophenyl)-5-(2,4-

disulfophenyl)-2H-tetrazolium, monosodium salt). WST-8 produces a water-soluble formazan dye upobioreductionon in the presence of an electron carrier, 1-Methoxy PMS (Figure 2.4).

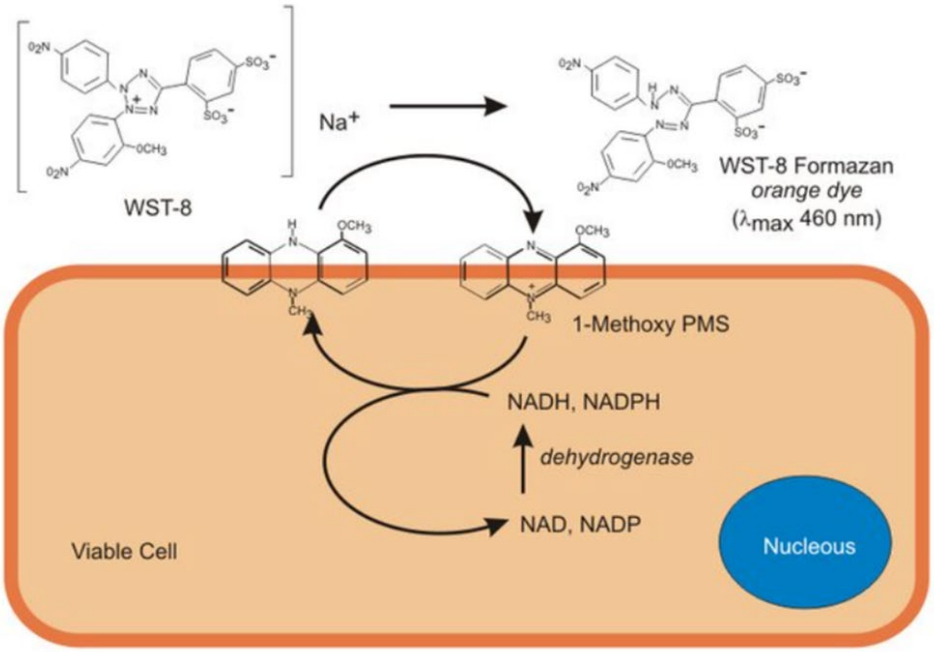

Figure 2.4. Metabolic activity of WST-8 with a viable cell to form formazan orange dye (Held 2009)

Proliferating cells show an increase in the activity of cellular dehydrogenases, which reduce WST-8 into an orange formazan product. After treatment with FSWP, 10 µl CCK-8 solution was added to the cells and incubated for 4 hours at 37 ºC. The formazan product was dissolved with 100 µl cell culture medium. The color change was detected at 460 nm with an ELISA plate reader. The number of living cells is directly proportional to the amount of formazan produced.

2.4. Cell cycle analysis & Annexin V-FITC/PI (propidium iodide) assay

Antiproliferative activity of FSWP on Caco-2 is further evaluated here to understand the mechanism behind cellular death.

2.4.1. Analysis of DNA fragmentation and cell cycle

Flow cytometry detects cell cycle-related molecular and metabolic changes by analyzing the expression of cell surface and intracellular molecules. In the principle of flow cytometry, the fluorescent PI is used to dye double-stranded DNA, and DNA fragmentation can be distinguished in cell cycle stages. At different cell cycle stages, the cells have an additional amount of DNA (Figure 2.5A). At the beginning of the cell cycle, a cell is in the G1 phase, where the growth is initiated for the cell to become larger. After the G1 phase, the cell gets into the S phase, where it starts replicating its DNA. So, the amount of DNA is doubled at the end of the S phase. During the M phase of the cell cycle, the cell segregates the chromosomes, and each daughter cell has a ploidy of N. In the flow cytometry diagram, the y-axis corresponds to the number of cells, and the x-axis shows the amount of DNA measured by fluorescence (Figure 2.5B).

Cells were seeded to a 6-well plate as 120000 cells/well and incubated for 18-24 h. Cells were synchronized with 1% FBS containing medium overnight. Treatment with 3000 µg/ml FSWP was performed and incubated for 72 hours. Control wells were given maintaining medium. Adherent and floating cells were collected with 10 minutes of centrifugation at 1200 rpm. Half of the population was taken for apoptosis analysis. The rest of the cell pellet was dissolved in 1ml cold PBS, and 4 ml of ice-cold ethanol was added while stirring at a low speed for the fixation. The fixed cell population was kept at -20 C^o at least for a day and up to 1 month. The cells were centrifuged at 4 Co and 1200 rpm on the analysis day for 10 minutes. The cell pellet was washed with cold PBS and dissolved in 1 ml of PBS containing 0,1% triton X-100. The samples were treated with 100 µl RNase A (200 µg/ml) (Macherey-Nagel, 740505.50) to remove double-stranded RNA from the samples and incubated for 30 minutes at 37 C^o. Then, 100 µl PI (1 mg/ml) (Sigma, P4170) was added and incubated for 15 minutes at room temperature. The fluorescent signal was collected to determine cell cycle stages in the population.

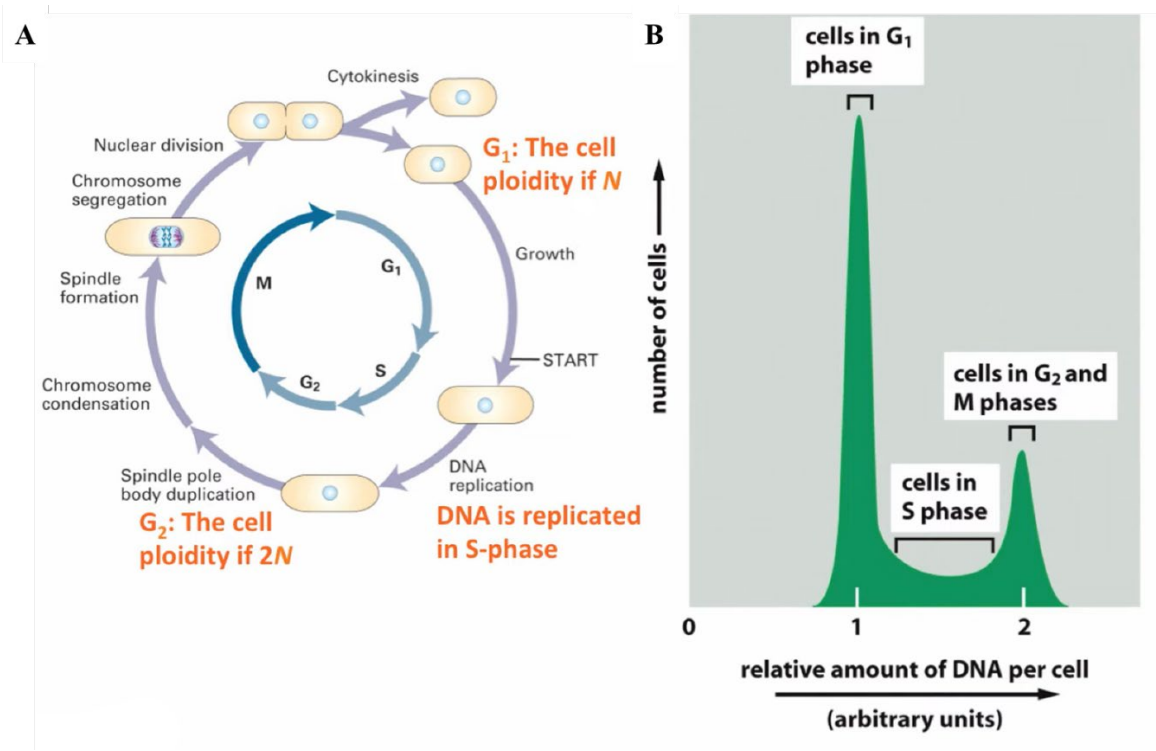

Figure 2.5. The amount of DNA in cell changes during the cell cycle; (A) Cell cycle stages; (B) Distribution of DNA levels in a heterogeneous population of cells

2.4.2. Apoptotic cell analysis (Annexin V-FITC/PI (propidium iodide) assay

Annexin V is an intracellular protein that binds to phosphatidylserine (PS) in a calcium-dependent manner. PS is a cell membrane component found on the intracellular leaflet in healthy cells. Early apoptotic cells lose their membrane asymmetry, and PS translocates to the external leaflet (Figure 2.6A). Thus, Annexin V can be used to identify and target apoptotic cells. PI is used as a counterstain to differentiate between necrotic and apoptotic cells. Early apoptotic cells cannot be stained with PI because their membrane integrity will still be rigid, and PI cannot reach DNA. However, late apoptotic and necrotic cells will be PI-positive (Figure 2.6B). Apoptotic and necrotic cells were detected using the FTIC Annexin V apoptosis detection kit (Biolegend, 640914). The cells were treated with FSWP at appropriate concentrations, and control cells were collected with an 800 rpm centrifuge for 5 minutes. The pellet was washed twice with PBS. Then, the cells were resuspended in Annexin V binding buffer provided in the kit

as 0.25-1.0*10^7 cells/ml. 5 µl of FTIC Annexin V was added per 100 µl of cell suspension. Also, 10 µl PI solution was added, and the cells were mixed with a gentle vortex. Incubation at dark was performed at room temperature for 15 minutes. 400 µl Annexin V binding buffer was added to each sample, and analysis was performed with flow cytometry.

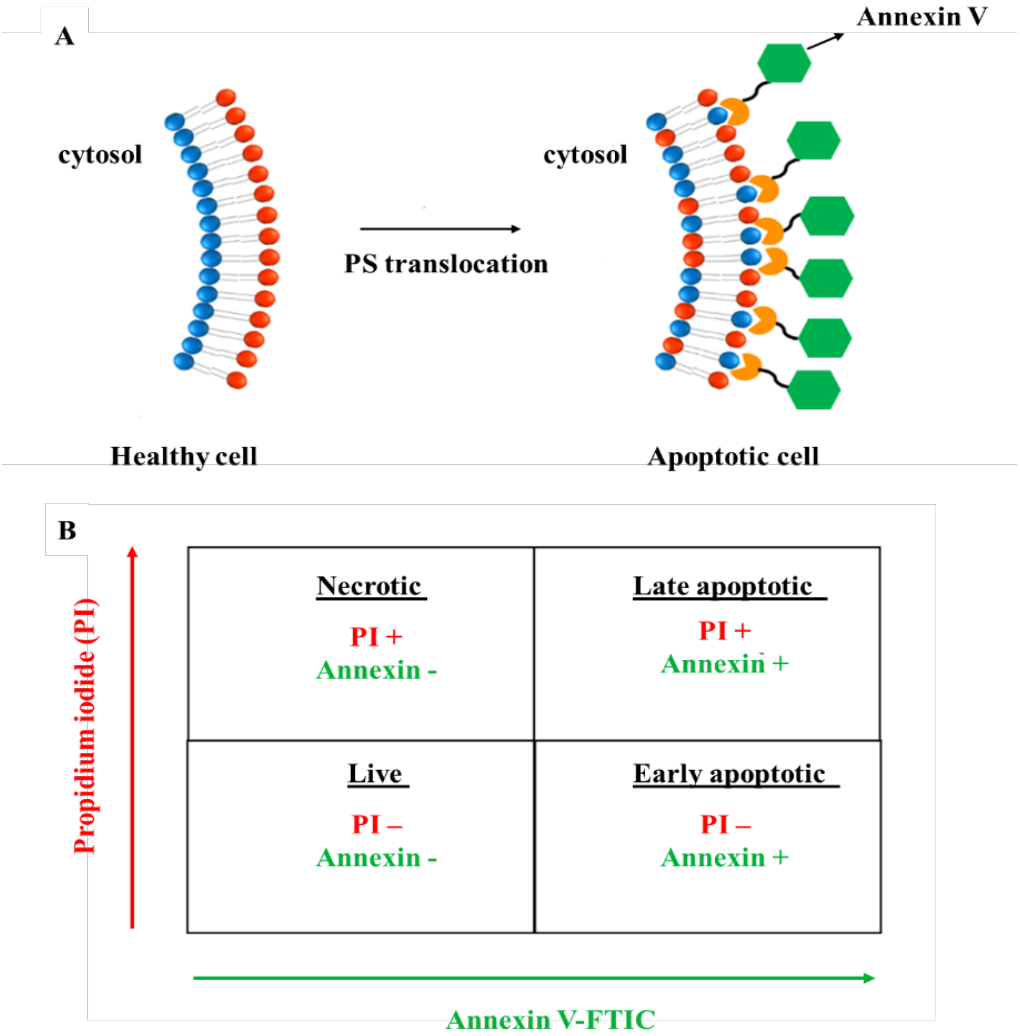

Figure 2.6. Apoptosis mechanism of action; (A) Phosphatidylserine (PS) translocation due to loss of plasma membrane asymmetry; (B) The expected staining illustration of apoptosis and necrotic cell population

2.5. 2-Deoxy glucose uptake colorimetric assay in Caco-2 uptake system

Most cells use glucose as the primary energy source, and there is a high regulation of glucose uptake into cells. GLUT family of transporters facilitates glucose uptake. Therefore, multiple mechanisms regulate sugar transporters' expression and activity. Glucose uptake was measured with a glucose uptake colorimetric assay kit (Sigma, MAK083). A glucose analog, 2-deoxyglucose (2-DG), is used to measure glucose uptake. 2-DG is taken up by cells and phosphorylated by hexokinase to 2-DG6P (Figure 2.7B**)**. 2-DG6P cannot be further metabolized and accumulates in cells as proportional to glucose uptake by cells. In the assay principle, 2-DG uptake is detected by a couple of enzymatic reactions. 2-DG6P is oxidized, generating NADPH that is utilized by glutathione reductase. A coupled enzymatic reaction produces glutathione that is reacted with DTNB to product TNB. TNB is detected at 412 nm in a spectrophotometer.

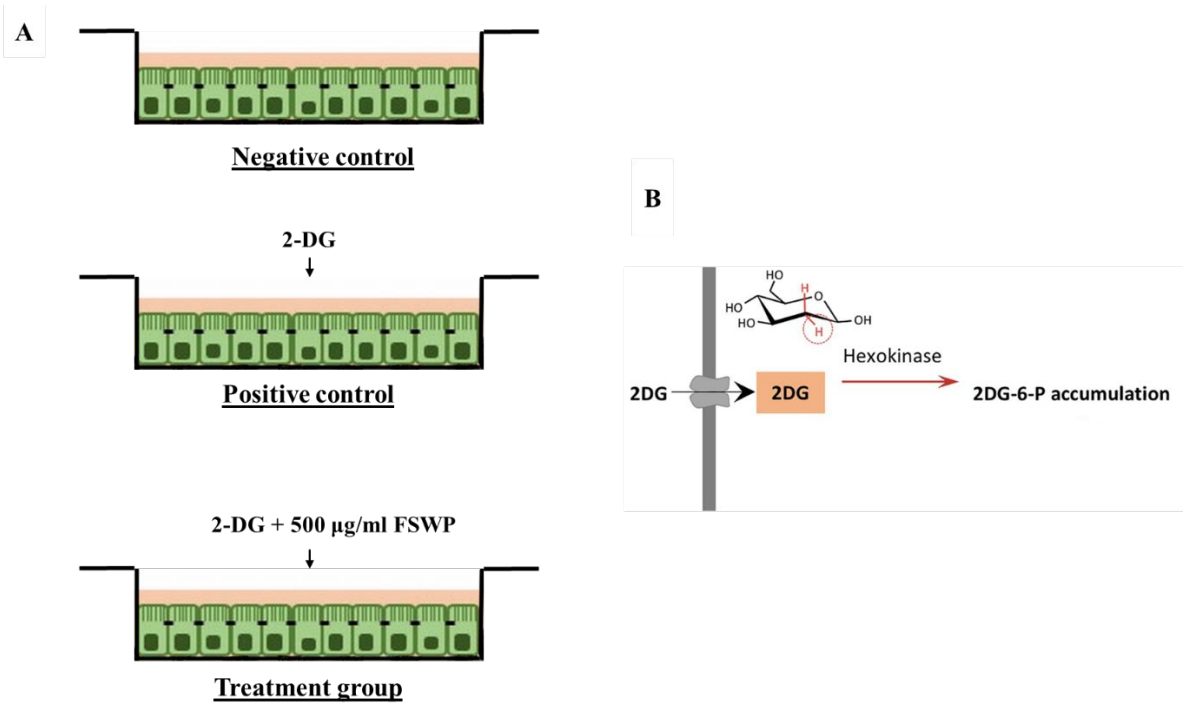

Figure 2.7. 2-Deoxy glucose uptake assay; (A) The experimental groups are shown as illustrations; (B) 2-DG is taken into the cell through glucose transporters and phosphorylated with hexokinase. 2-DG6P accumulates inside the cell.

2.5.1. 2-Deoxy glucose uptake experiment and sample collection

Cells were seeded in 96 well plates at a density of 4000 cells/well containing 250 µl culture medium in each well. After confluency, their medium was replaced every 2 days up to 14 days. The 14 days old monolayers were washed with PBS twice, and DMEM medium without D-glucose, L-glutamine, sodium pyruvate, and phenol red were exposed to the cells for glucose starvation for 60 minutes. After washing the monolayers with PBS twice, the negative control, positive control, and treatment groups were exposed to KREBS buffer for 30 minutes. The experimental groups are demonstrated in Figure 2.7A. KREBS buffer was removed from the treatment group and replaced with 500 µg/ml FSWP dissolved in KREBS buffer. 10 µl of 2-deoxyglucose was introduced to the positive control and treatment group and incubated for 30 minutes. After monolayers were washed 3 times with PBS, cells were lysed with 80 µl extraction buffer. Lysates were freeze-thawed in liquid nitrogen for a few minutes and heated to 85 ^{o}C for 40 minutes. Then lysate was cold on ice for 5 min, and 10 µl neutralization buffer was added. The lysate was centrifuged at 13000g for 1 min, and 5 µl supernatants were diluted with 45 µl of assay buffer and used as a sample for colorimetric analysis. In contrast, 50 µl assay buffer was used as a blank.

2.5.2. 2-Deoxy glucose standard curve

10 mM 2-DG6P standard solution was diluted to form 0.01 mM in an appropriate volume. Up to 100 pmole/well, standards were run in duplicate. The samples and standards were replaced into 96 well plates and proceeded to assay reaction. The background (0 2-DG6P std) was subtracted from all std readings, and absorbance at 412 nm (y-axis) vs. pmole of 2-DG6P (x-axis) was a plot for the standard curve (Appendix A).

2.5.3. Assay reaction

Reaction mix A containing enzyme mix for NADPH generation was prepared, and 10 µl of reaction mix A added to each well by pipetting. The plate was covered and incubated at 37 ºC for 60 minutes in the dark. 90 µl extraction buffer was added to each well to degrade NADP. The plate was sealed and heated to 90 ºC for 40 minutes. It was cool on ice for 5 minutes, and then 12 µl neutralization buffer was added. Reaction mix B was prepared with 20 µl glutathione reductase, 16 µl substrate-DTNB, and 2 µl recycling mix per well. Reaction mix B was added to each well as 38 µl and mixed by pipetting. The absorbance was collected at 412 nm every 5 minutes in an ELISA microplate reader maintained at 37 ºC. The endpoint reading was decided when 100 pmole standards reached 1.5-2.0 OD. For samples, assay buffer was used as background, and 2-DG6P present in the samples determined from the std curve as proportional to 2-DG taken up by cells.

2.6. Testing FSWP as a functional food ingredient

In this part of the thesis, the effect of FSWP on glucose absorption is aimed to be modeled on the intestinal enterocyte transport system. The biological health potential of FSWP as an additive to a food product containing glucose is demonstrated by adding it into yogurt. Firstly *in vitro* digestion protocol was applied to samples and control groups to mimic the human digestive tract. Then, the samples were tested for bio-accessible glucose. After, intestinal cell monolayers were treated with samples and controls from the apical side of the system. Glucose efflux sampling was performed from the basolateral side of the system, and they were quantified for bioavailable glucose.

2.6.1. *In vitro* test tube digestion

Low-fat yogurt was obtained from SÜTAŞ commercially and lyophilized to have a uniform and stable test material. The amounts of samples for *in vitro* digestion were determined based on dry matter of yogurt and toxicity of glucose and FSWP Caco-2 cells.

The lyophilized yogurt, FSWP, and glucose samples were combined in different orders to model the functionality of the digestive system (Figure 2.8). The gastric fluid solution was prepared with 1% g (w/v) pepsin, 1% g (w/v) guar gum, and 0.05 M HCl (v/v) in 50 mL water. The lyophilized yogurt (0.4 g), FSWP (0.025 g), and glucose (0.28 g) samples were added to each mentioned combination to 5 mL of gastric fluid solution and incubated for 30 min at 37°C. 5 mL of sodium acetate solution (0.25 M) was added to neutralize the pH. Intestinal fluid was prepared with 3 g pancreatin in 20 mL water and vortexed for 10 minutes. The pancreatic enzyme solution was centrifuged at 4500 rpm for 10 min. 15 mL supernatant was placed into a new tube and combined with 0.666 mL amyloglucosidase and 1 mL (10 mg/mL) invertase enzymes. The intestinal digestion phase was started by adding 2.5 mL intestinal fluid mixture and five glass balls into the samples from the gastric digestion. The mixtures were incubated for two h at 37°C and 100 rpm in an orbital shaker. The samples were lyophilized for further experiments.

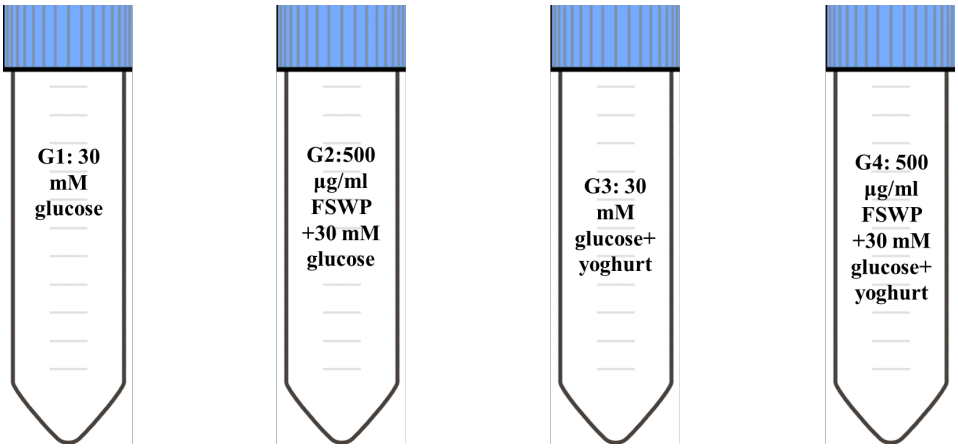

Figure 2.8. The combinations of experimental samples for *in vitro* digestion

2.6.2. Glucose standard curve

Glucose quantification was performed with an enzymatic glucose assay kit (Sigma, GAGO20). Enzymatic methods are sensitive and specific analytical tools. In the principle of the assay, D-glucose is converted into D-gluconic acid and hydrogen peroxide with glucose oxidase. Produced hydrogen peroxide is reacted with colorless o-dianisidine to oxidize it to brown o-dianisidine in the presence of peroxidase. Brown

product reacts with sulfuric acid to form a more stable, pink-colored product, o-dianisidine. The intensity is measured at 540 nm, that is proportional to the original glucose concentration. D-glucose standard (1 mg/ml) was prepared in appropriate volumes and concentrations to run in duplicate. Each std was distributed to 96 well microplates, and a 100 µl assay reagent containing glucose oxidase/peroxidase reagent and o-dianisidine was added. The reaction was incubated at 37°C for 30 minutes. Then, the reaction was stopped by adding 100 µl 6 M H_2SO_4 into each well. The absorbance was measured at 540 nm against the reagent blank. Absorbance at 540 nm (y-axis) vs. mg of glucose (x-axis) was plotted for the standard curve (Appendix B).

2.6.3. Bioaccessibility of glucose after *in vitro* digestion

A glucose assay was performed after in vitro digestion to determine bioaccessible glucose in each group.

2.6.4. Glucose absorption experiment and bioavailability of glucose

Caco-2 cells were grown on 12- well inserts for 21 days to differentiate to form enterocyte morphology. TEER was measured to check monolayer integrity and polarized structure. The digested samples were dissolved in KREBS transport buffer and introduced to the apical side of the transport systems. Glucose (30 mM) and FSWP (500 µg/ml) amounts were standardized in each sample (Figure 2.9). The samples were collected from the basolateral side at 30, 60, 90, 120, and 150 mins. Glucose assay kit (GO Assay Kit, Sigma-Aldrich, GAGO20) was used to quantitate glucose efflux for each time point.

2.7. Statistical Analysis

Data were expressed as mean ± standard error. Student's t-test and one-way ANOVA analyzed the data. P-value < 0.05 was considered statistically significant. Statistical analysis was performed using the Graphpad Prism 7.0 software.

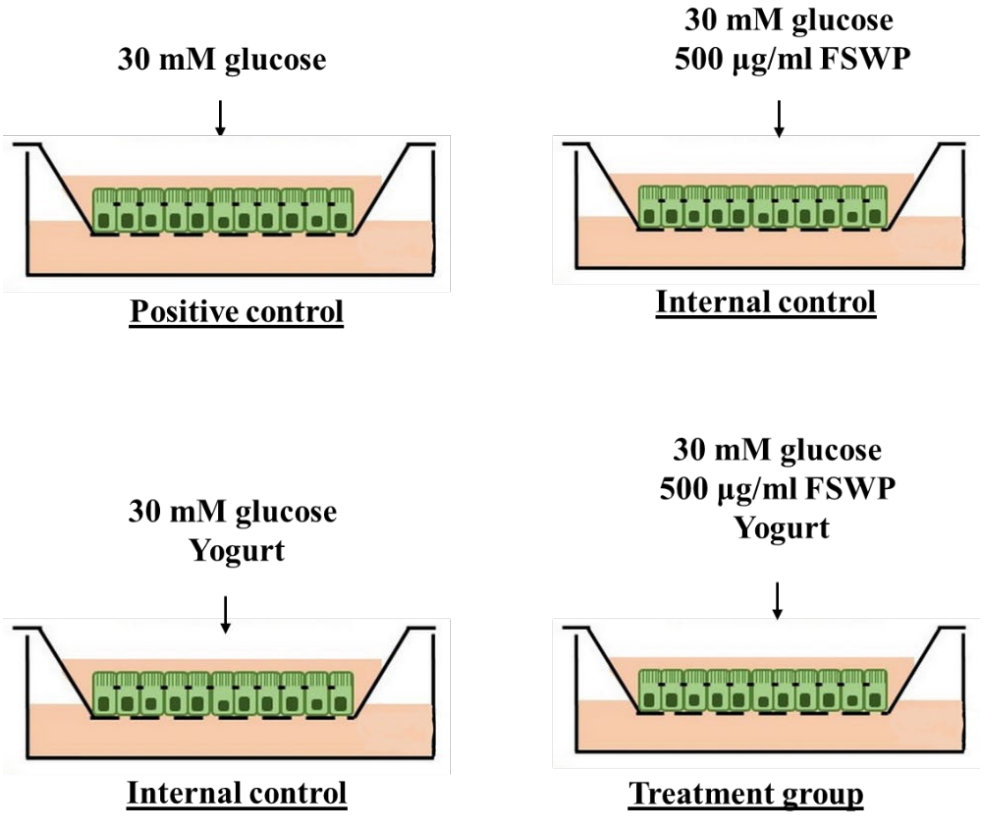

Figure 2.9. Glucose absorption experimental set-up

CHAPTER 3

RESULTS AND DISCUSSION

3.1. Anticarcinogenic activity of FSWP

3.1.1. The cellular toxicity of FSWP

The cellular toxicity of FSWP on the Caco-2 cell line was analyzed in this part of the thesis. The concentrations of up to 3000 µg/ml FSWP were treated to Caco-2 cells for the following 72 hours. Control cells reached 85-90% confluency at the end of the treatment (Figure 3.1A).

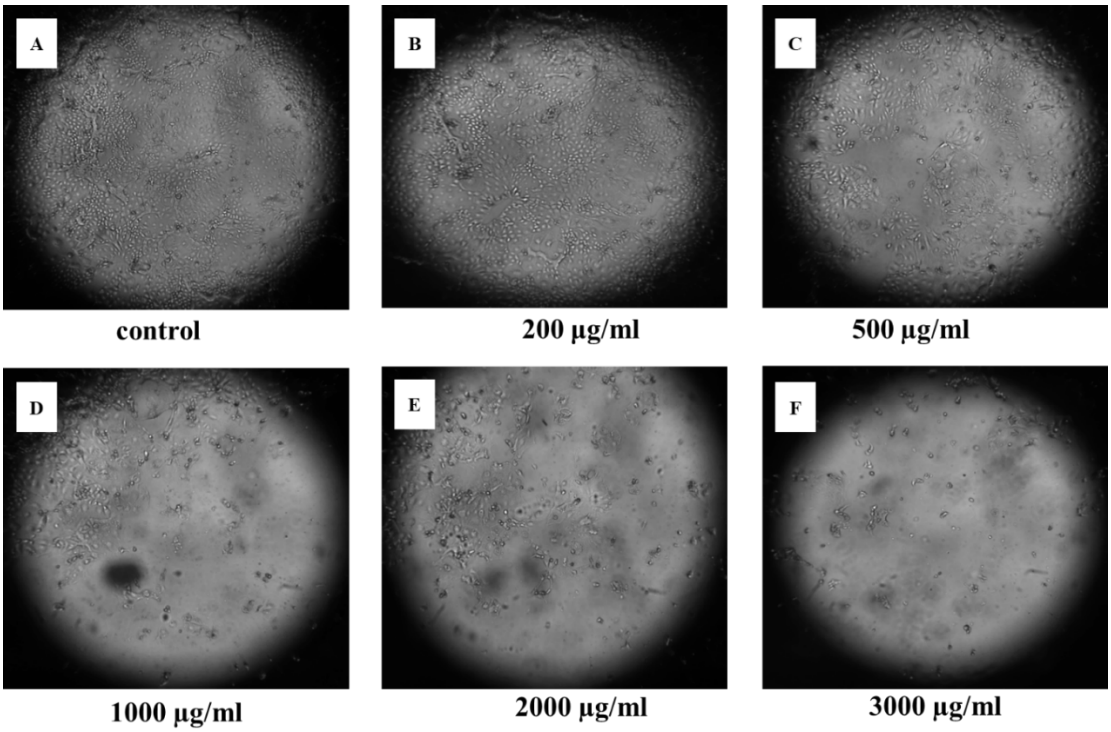

Figure 3.1. Images of colon cancer cell line, Caco-2 treated with FSWP for 72 hours; (A) Caco-2 control; (B) 200 µg/mL FSWP; (C) 500 µg/mL FSWP; (D) 1000 µg/mL FSWP; (E) 2000 µg/mL FSWP; (F) 3000 µg/mL FSWP (100X magnification)

FSWP treatment groups at 200 μg/ml and 500 μg/ml concentrations showed a similar proliferation pattern to the control group (Figure 3.1.). However, the cells treated with 1000 μg/ml FSWP and higher exhibit inhibition of cellular growth, and cellular toxicity increases proportionally with concentrations of FSWP (Figure 3.1.). The observations made under the microscope were validated with the enzymatic wst-8 cytotoxicity assay. As seen in Figure 3.2, cell proliferation is inhibited significantly starting with 1000 μg/ml FSWP, and cell viability is decreased proportionally with increasing FSWP concentration ($p<0.05$). FSWP reveals antiproliferative activity by reducing the cellular growth of Caco-2 colon cancer cells.

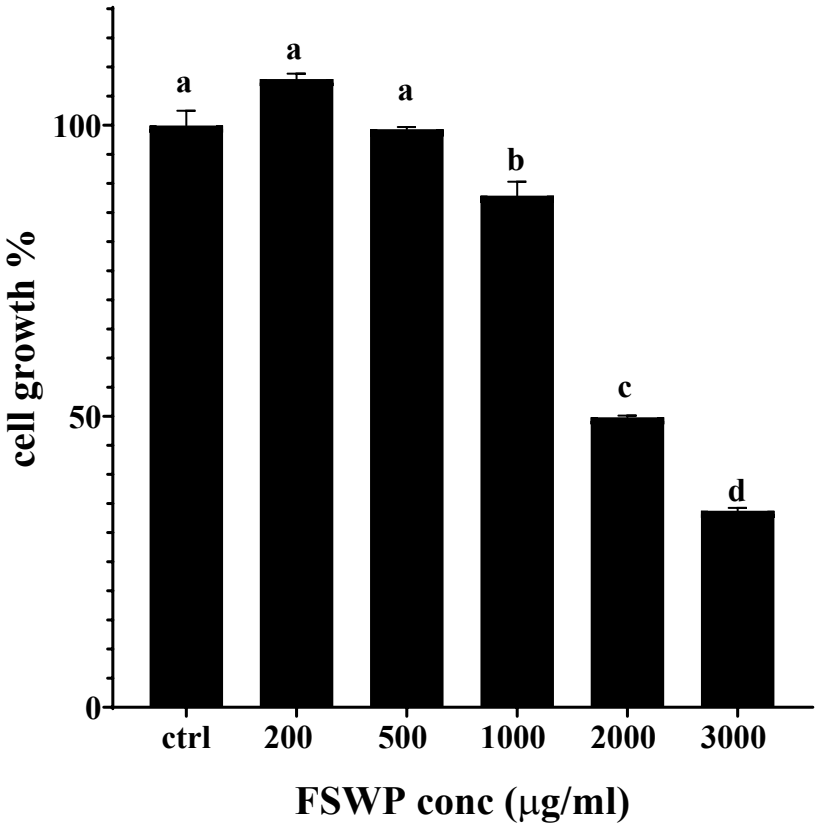

Figure 3.2. FSWP inhibited the survival of Caco-2 cell line. Cell growth was detected with WST-8 cytotoxicity assay after 72 hours of treatment of FSWP at indicated concentrations. Results represented mean ± standard deviations of independent triplicates expressed as a percentage relative to control. Letters indicate statistically significant differences between concentrations and control at $p \leq 0.05$.

3.1.2. Effect of FSWP on cell cycle distribution

Flow cytometry analysis was performed to detect cell cycle profiles of FSWP-treated Caco-2 cells for 72 hours. Untreated cells were used as control. The bar shows representative cell cycle plots of control and treatment cells and the graphical representation of G0/G1, S, and G2/M (Figure 3.3).

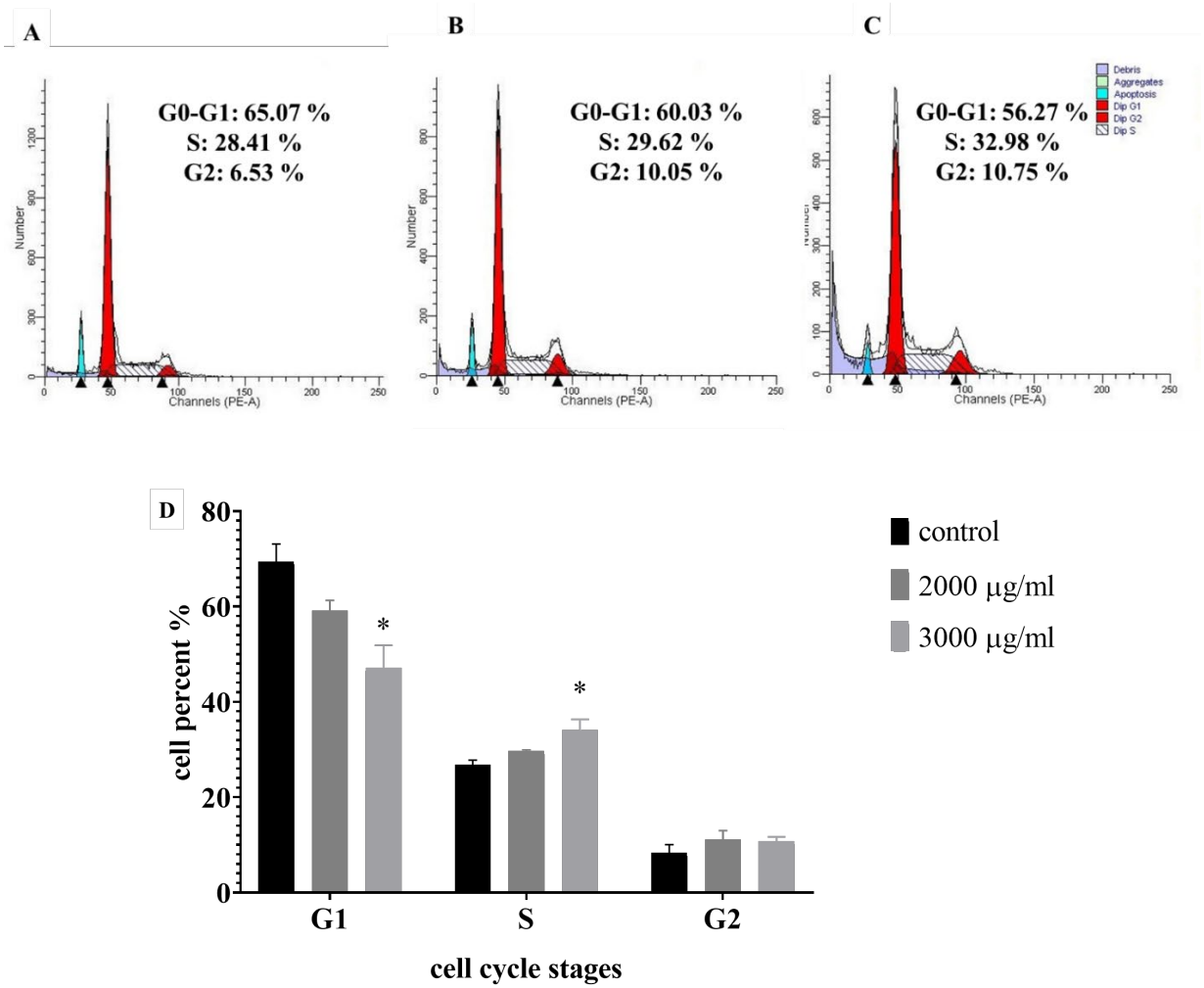

Figure 3.3. Cell cycle analysis through PI staining and following flow cytometry for Caco-2 cells after FSWP treatments. The quantitative measurement of cell cycle phase. (A) Caco-2 control; (B) 2000 µg/mL FSWP; (C) 3000 µg/mL FSWP; Data are representatives of three independent experiments with similar results. (D) The bar diagram represents % of cells in the cell cycle's G1, S, and G2/M phases AND significant differences are denoted by * ($p < 0.05$).

The percentage of cells was statistically compared with the untreated control group in each cell cycle stage. The highest dose of FSWP induced a significant reduction in the number of cells in the G_0/G_1 phase fraction from 65.07 % in control to 56.27 %. Also, there is a significant increase in cell population in the S phase in the 3000 µg/ml FSWP treated cell population compared with that in the control group. Results indicate that there is an S phase arrest at 72 h post-FSWP. Therefore, FSWP may mediate the anticancer effect by inhibiting cell proliferation and cell cycle arrest.

3.1.3. Effect of FSWP on apoptosis-inducing ability

The observed decline in cell viability in cytotoxicity assay could be related to the apoptotic effect of FSWP. To test the apoptotic effect, Annexin V/PI staining was performed after 3000 µg/ml FSWP treatment for 72 hours. Representative apoptosis plots are given in figure 3.4A. Q1 region in the AnnexinV/PI plot shows the dead or necrotic cells that are not intact anymore. FSWP treatment causes a more significant amount of necrotic Caco-2 population. Q2 region represents late apoptotic cells covering a greater number of cells in the FSWP treatment group than in control. Therefore, fewer healthy cell populations exist in the treatment group and Q3 regions of the plots. The cells in the Q4 portion are early apoptotic, which does not reach a significant number in treatment. Annexin V/PI flow cytometric measurements reveal a significant increase in late apoptotic and necrotic cells of the FSWP treatment group compared to the control group in figure 3.4B. Hence, the results showed the ability of FSWP to inhibit colon cancer cell growth and induce S-phase arrest followed by apoptosis in Caco-2 cells.

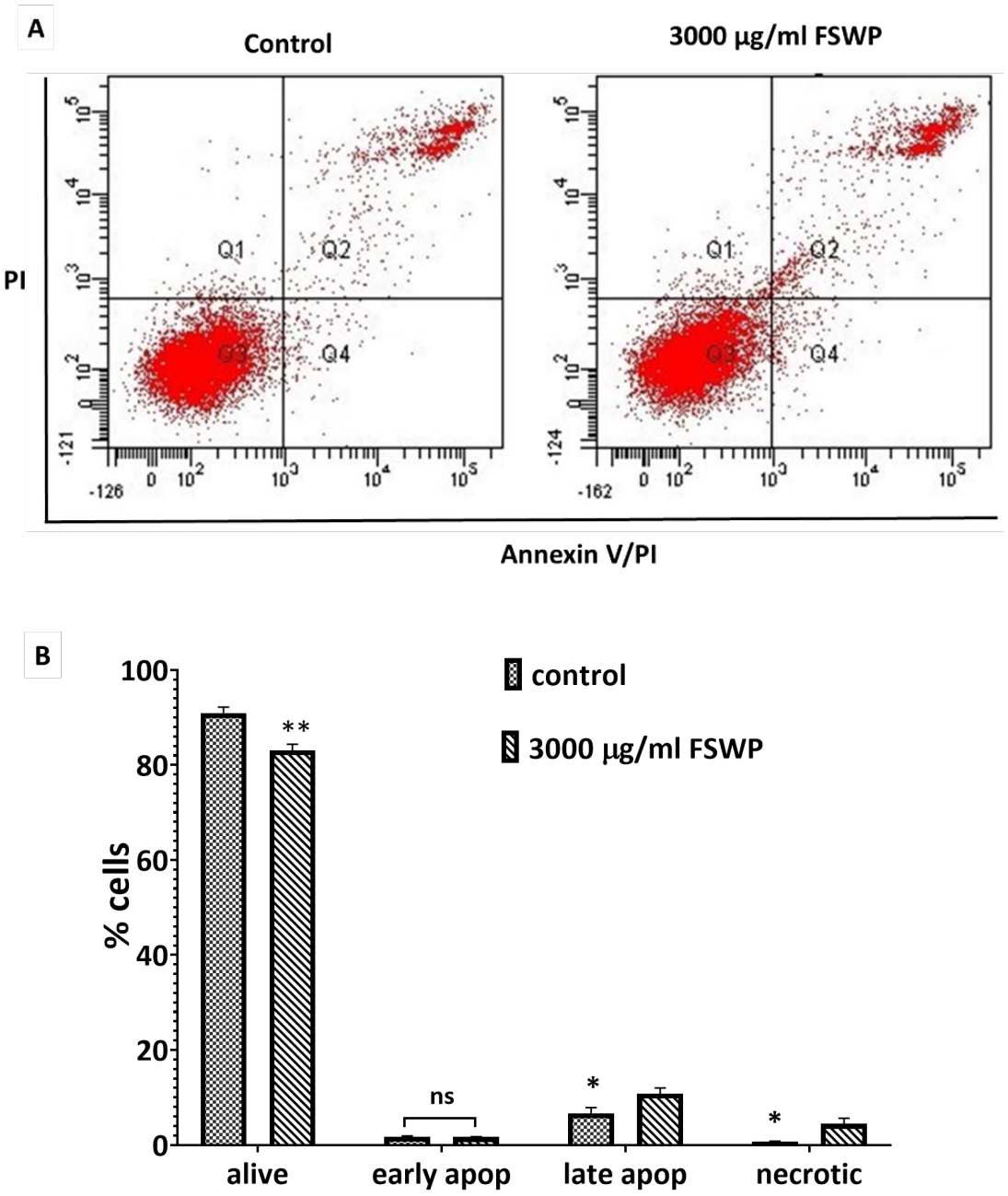

Figure 3.4. Caco-2 cells were treated with FSWP for 72 h and stained with Annexin V-FITC/PI for flow cytometric analysis. (A) Representative flow cytometry plots using Annexin V-FITC/PI staining for apoptosis. (B) The percentage of apoptotic cells was statistically compared with an untreated control group, and significant differences are denoted by * ($p < 0.05$). Experiments are performed in triplicate, and data are expressed as the mean ± standard error of the mean (SEM).

3.2. Effects of FSWP on 2-Deoxy-Glucose Uptake in Caco-2 Cell

This part of the thesis is aimed to investigate the effect of FSWP on glucose uptake of intestinal enterocyte cell model, Caco-2. For this purpose, the highest non-toxic concentration of FSWP (500 μg/ml) was applied on Caco-2 cells with the glucose analog, 2-DG, and the cells treated with only 2-DG was used as a positive control. The effect of FSWP on systemic glucose uptake is demonstrated in figure 3.5. The treatment group shows a significant reduction in glucose uptake compared to the positive control ($p<0,05$). The relative 2-DG amount shows that there is around 25% reduction in FSWP treatment group compared to control (Figure 3.5B).

Therefore, FSWP has an inhibitory effect on glucose entry into cells. Negative control cells have a lower amount of 2-DG due to the basal level of NADPH in metabolism. This experiment demonstrated the direct interaction of FSWP on glucose uptake of intestinal epithelial cells. Hasegawa showed that lignosulfonic acid, a lignin derivative had an inhibitory impact on 2-deoxyglucose uptake of Caco-2 cells (Hasegawa et al., 2015). Administration of FSWP with 2-DG interfered with glucose uptake by inhibiting glucose transport.

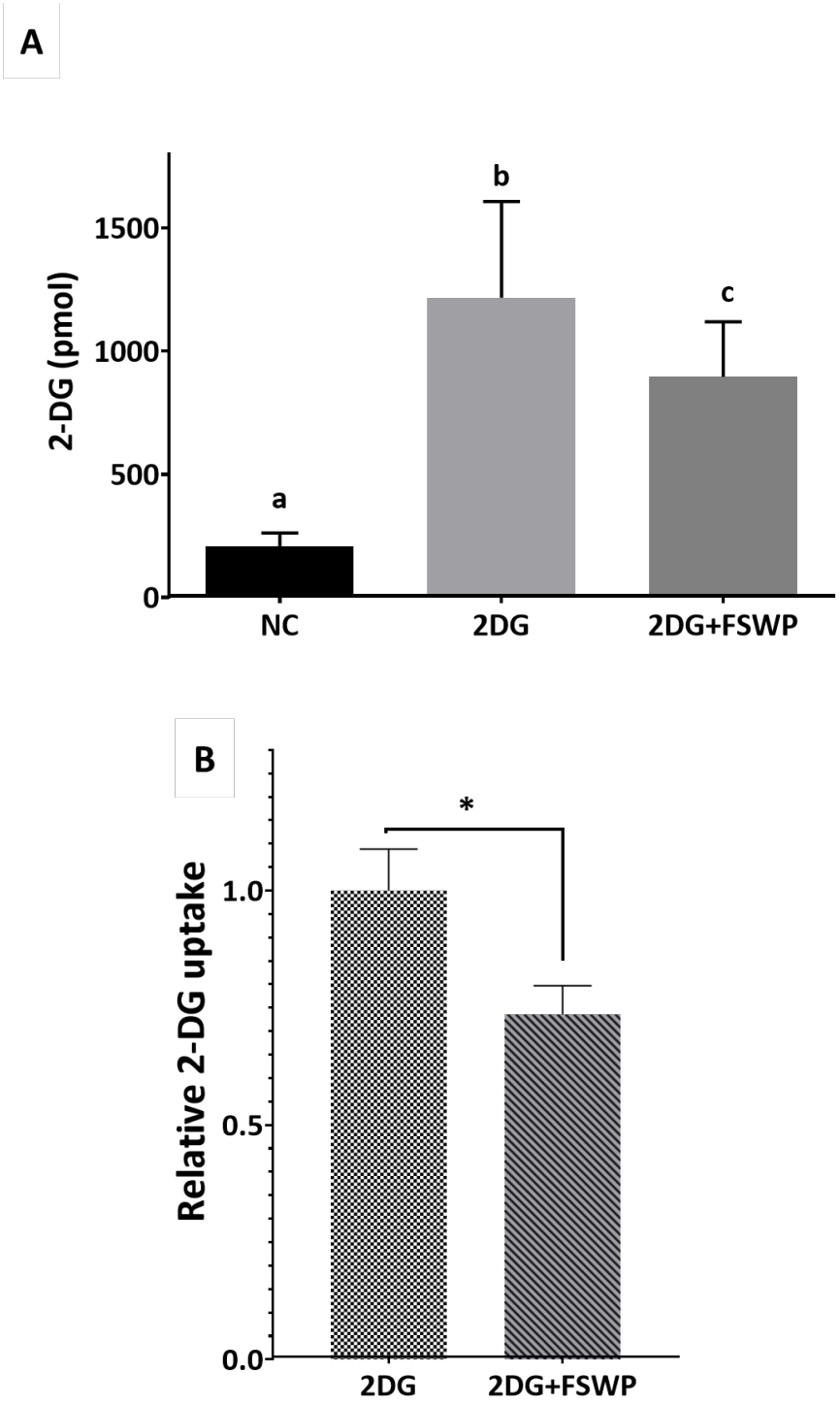

Figure 3.5. Effect of FSWP on 2-DG uptake in Caco-2 cells (A) The statistical significance was determined by one-way ANOVA with Tukey's test ($p < 0.05$). Letters indicate statistically significant differences at $p \leq 0.05$. (B) The amount of 2-DG uptake is shown as relative 2-DG uptake compared with that in the absence of FSWP. The statistical significance was determined by an unpaired t-test test, and significant differences are denoted by * ($p < 0.05$).

3.3. Glucose Absorption from FSWP Supplemented Yogurt

Dietary fibers have been associated with an impact on the activity of digestion enzymes (Schneeman and Gallaher 1985; Qi, Al-Ghazzewi, and Tester 2018). The colloidal structure formed by dietary fibers could physically affect enzyme-substrate interaction. Bio-accessible glucose levels were determined after in vitro digestion to compensate for the effect on enzyme activity. There is no significant difference between G and PG, YPG and YG for glucose levels (Figure 3.6).

It presents that FSWP and/or yogurt did not affect *in vitro* digestion enzyme activity in the case. Therefore, the availability of glucose for absorption can be counted as the same for all experimental groups.

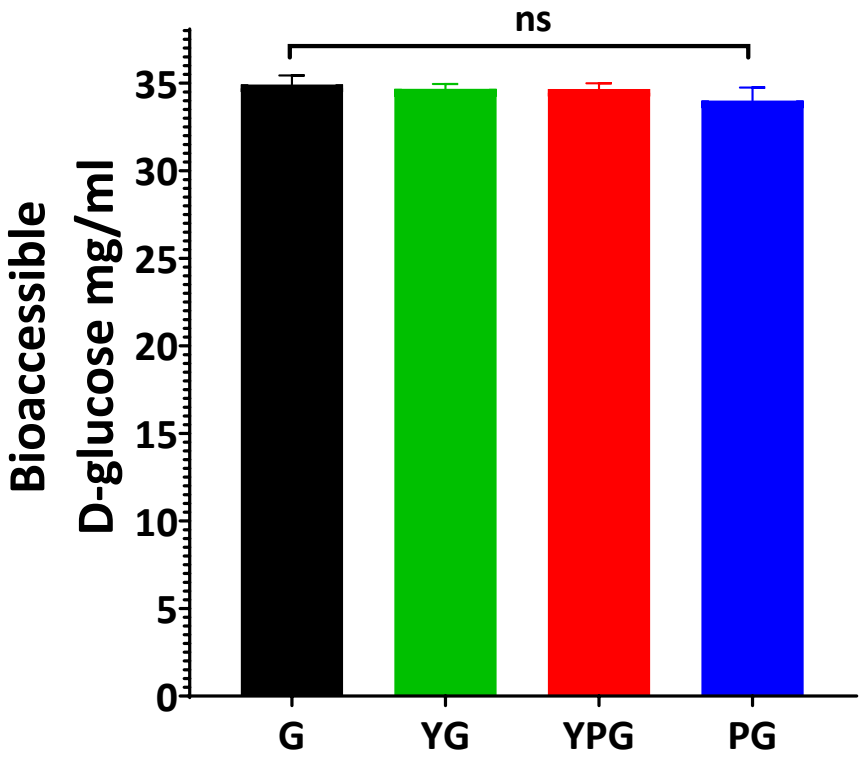

Figure 3.6. Glucose bioaccessibility after *in vitro* digestion of experimental controls and treatment groups. G: glucose; PG: pectin+glucose; YPG: yogurt+pectin+glucose; YG: yogurt+glucose. Data represented as mean ± SEM.

The rate of glucose efflux through enterocyte cells is relevant to physiology. For instance, functional food design focuses on producing functional foods with a lower glucose absorption rate. To test the potency of FSWP as a bioactive ingredient, FSWP's effect on glucose absorption was displayed by adding FSWP into yogurt with glucose. Lyophilized experimental samples were given to the apical side of Caco-2 monolayers containing 500 μg/ml FSWP and 30 mM glucose. Samples were collected from the basolateral side for up to 120 minutes in a 30 min interval. It is possible that glucose absorption continued for 120 minutes with increased glucose on the basolateral side.

Positive control containing only glucose (G) has the highest amount of glucose at 30, 90, and 120 minutes. The experimental group containing yogurt, FSWP, and glucose (YPG) has the lowest amount of glucose at 30, 90, and 120-time points compared to the internal control containing yogurt and glucose (YG). Thus, FSWP caused a statistically significant reduction in glucose absorption in the enterocyte cell model for a total of 120 minutes. When the glucose levels at 30 minutes are compared, the glucose efflux goes as YPG, PG, YG, and G from lowest to highest. Internal control PG showed a significant reduction in glucose release at 30 minutes compared to G. The decline is greater in YPG compared to both G and YG. Thus, FSWP decreased glucose absorption through the Caco-2 transport system for the following 30 minutes after treatment. The glucose levels at 60 minutes are similar in all the groups. This might be caused by a compensatory effect of the glucose transporters due to a molecular response. They may reach a saturation level by glucose, leading to a stable glucose transport rate. The molecular mechanism behind this effect at a particular time point needs further investigation. The inhibitory effect of FSWP on glucose absorption is reached at a significant level after 90 minutes when YPG is compared with G and YG. Also, YPG kept inhibiting glucose release for up to 120 minutes, and there was a significant reduction in glucose levels in YPG compared to both G and YG. Overall glucose efflux through 120 minutes time period is seen in figure 3.8A.

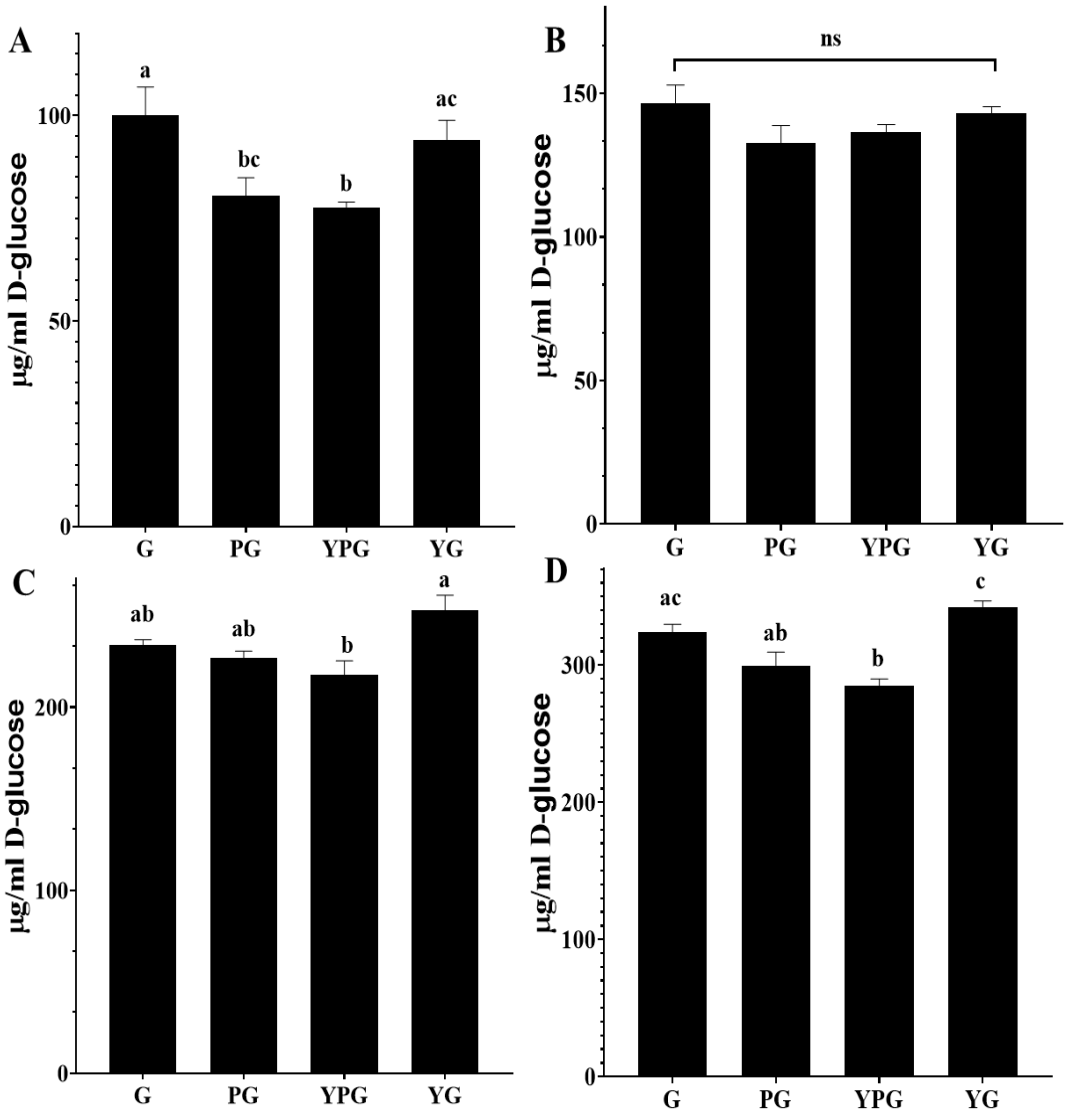

Figure 3.7. Glucose bioavailability and transport through Caco-2 cells. G: glucose; PG: pectin+glucose; YPG: yogurt+pectin+glucose; YG: yogurt+glucose (A) 30 minutes; (B) 60 minutes; (C) 90 minutes; (D) 120 minutes. Results presented as mean glucose concentration of independent triplicates ± standard error mean. Letters represent statistically significant differences between control and experimental groups at $p \leq 0.05$.

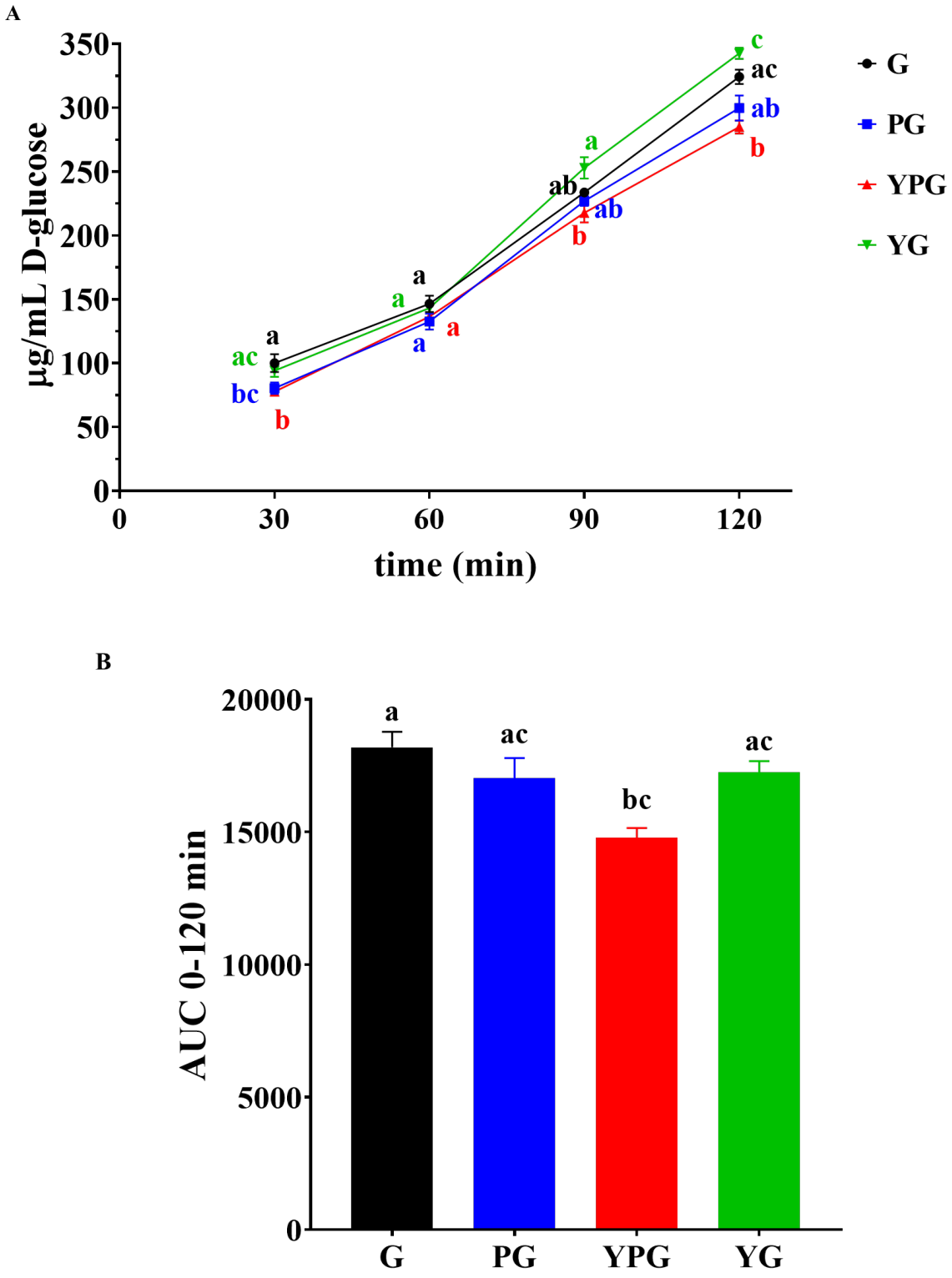

Figure 3.8. Glucose availability and transport through Caco-2 enterocyte cell model. G: glucose; PG: pectin+glucose; YPG: yogurt+pectin+glucose; YG: yogurt+glucose; (A) Glucose time course; (B) Area under the curve (AUC)

CHAPTER 4

CONCLUSION

Our studies reveal the biological activity of fig stalk waste pectin (FSWP) on colon cancer cell growth and intestinal glucose absorption *in vitro*.

The first section of the FSWP health effects aims to understand the impact on colon cancer cell growth. FSWP showed an antiproliferative effect on colon cancer Caco-2 cell line. Firstly, it was found that FSWP suppressed the survival of Caco-2 at concentrations starting with 1000 μg/ml, and the inhibitory effect was increased proportionally to increasing concentration. FSWP exhibited promising cytotoxicity toward the colon cancer cell line. Bergman (2010) showed that citrus pectin inhibits cell proliferation in 3 different cancer cell lines, HuCC, HT-29, and K562 but not in Raji cells (Bergman et al. 2010). The three cell lines affected are known to express Gal-3, while Raji cells do not express Gal-3. They proposed that antiproliferative activity might be triggered by the interaction of citrus pectin with Gal-3. It is known that Gal-3 is highly expressed in the Caco-2 cell line. Furthermore, cell cycle analysis was performed to understand the potential mechanism by which FSWP inhibited cellular proliferation. The results suggest that FSWP disturbs cell cycle progression and leads to the accumulation of cells in the S phase. The passage through the cell cycle cannot be regulated properly due to the loss of cell cycle checkpoints. Cancer cells proliferate relentlessly when checkpoints cannot monitor cell cycle progression. DNA integrity and gene expression could be defected due to the loss of checkpoints. Therefore, FSWP acted by inducing S cycle arrest and leads to inhibition of growth of Caco-2 colon cancer cells. The reason behind the reduction in cell survival could be the apoptosis-inducing ability of FSWP. The apoptosis analysis showed an increase in the late apoptotic and necrotic cell population due to FSWP treatment. This suggests that FSWP inhibited cell growth through the induction of apoptosis. The anticancer effect of FSWP is mediated by the inhibition of proliferation, inducing cell cycle arrest and apoptotic cell death.

In the second section of the thesis, FSWP is evaluated in terms of anti-diabetic characteristics. Caco-2 uptake system is combined with 2-deoxyglucose to demonstrate glucose uptake from the lumen of the small intestine by enterocyte cells. We found that

FSWP inhibited glucose uptake into Caco-2 cells from the apical compartment. It triggered a reduction in glucose entry and showed anti-diabetic features.

In the last part of the thesis, FSWP's potential as a food ingredient is demonstrated in a food application. It is added into yogurt as a dietary supplement, and the glucose efflux is modeled in the Caco-2 transport system. The glucose amount given to the basolateral side for 120 minutes is lower in the YPG food application group compared to positive (G) and internal controls (YG and PG). The impact seems to be time-dependent, which gives a clue about the molecular response due to saturation levels of glucose transporters. The dynamic response to glucose efflux lasted for 120 minutes in the Caco-2 transport system. The internal control (PG) in food application experimental design also showed that FSWP had a lowering impact on glucose release to the basolateral side compared to G. These results overlap with the findings in 2-DG glucose uptake experiments. Both show that glucose absorption in the intestine is affected due to FSWP addition *in vitro*. Several studies revealed that pectin positively impacts the decrease in blood glucose levels. Pectin isolated from *Passiflora glandulosa* was fed to diabetic mice for 30 days, and the animals showed improved hypoglycemic action by reducing blood glucose levels (Sousa et al. 2015). Also, pectin-rich polysaccharides from unripe apples showed enhanced glucose metabolism in healthy volunteers (Makarova et al., 2015). Glycemic response by pectin is correlated with the triggered reduction in intestinal glucose absorption due to high viscosity and chemical characteristics (Wicker et al., 2014). Our findings support the effect of FSWP on lowering glucose absorption in the intestine.

REFERENCES

Adam, Clare L, Lynn M Thomson, Patricia A Williams, and Alexander W Ross. 2015. "Soluble Fermentable Dietary Fibre (Pectin) Decreases Caloric Intake, Adiposity and Lipidaemia in High-Fat Diet-Induced Obese Rats." *PloS One* 10 (10): e0140392.

Bandazhevskaya, Galina S, Vassily B Nesterenko, Vladimir I Babenko, I v Babenko, T v Yerkovich, and Y I Bandazhevsky. 2004. "Relationship between Caesium (137cs) Load, Cardiovascular Symptoms, and Source of Food in" Chernobyl" Children-Preliminary Observations after Intake of Oral Apple Pectin." *Swiss Medical Weekly* 134 (49–50): 725–29.

Bergman, M, M Djaldetti, H Salman, and H Bessler. 2010. "Effect of Citrus Pectin on Malignant Cell Proliferation." *Biomedicine & Pharmacotherapy* 64 (1): 44–47.

Brouns, F, E Theuwissen, A Adam, M Bell, A Berger, and R P Mensink. 2012. "Cholesterol-Lowering Properties of Different Pectin Types in Mildly Hyper-Cholesterolemic Men and Women." *European Journal of Clinical Nutrition* 66 (5): 591–99.

Brown, Lisa, Bernard Rosner, Walter W Willett, and Frank M Sacks. 1999. "Cholesterol-Lowering Effects of Dietary Fiber: A Meta-Analysis." *The American Journal of Clinical Nutrition* 69 (1): 30–42.

Candogan, Kezban, and Nuray Kolsarici. 2003. "The Effects of Carrageenan and Pectin on Some Quality Characteristics of Low-Fat Beef Frankfurters." *Meat Science* 64 (2): 199–206.

Chen, Chien-Ho, Ming-Thau Sheu, Tzeng-Fu Chen, Ying-Ching Wang, Wen-Chi Hou, Der-Zen Liu, Tsao-Chuen Chung, and Yu-Chih Liang. 2006. "Suppression of Endotoxin-Induced Proinflammatory Responses by Citrus Pectin through Blocking LPS Signaling Pathways." *Biochemical Pharmacology* 72 (8): 1001–9.

Cheng, Hairong, Shanshan Li, Yuying Fan, Xiaoge Gao, Miao Hao, Jia Wang, Xiaoyan Zhang, Guihua Tai, and Yifa Zhou. 2011. "Comparative Studies of the Antiproliferative Effects of Ginseng Polysaccharides on HT-29 Human Colon Cancer Cells." *Medical Oncology* 28 (1): 175–81.

Delphi, Ladan, and Houri Sepehri. 2016. "Apple Pectin: A Natural Source for Cancer Suppression in 4T1 Breast Cancer Cells in Vitro and Express P53 in Mouse Bearing 4T1 Cancer Tumors, in Vivo." *Biomedicine & Pharmacotherapy* 84: 637–44.

D'Souza, Warren N, Jason Douangpanya, Sharon Mu, Peter Jaeckel, Ming Zhang, Joseph R Maxwell, James B Rottman, Katja Labitzke, Angela Willee, and Holger Beckmann. 2017. "Differing Roles for Short Chain Fatty Acids and GPR43 Agonism in the Regulation of Intestinal Barrier Function and Immune Responses." *PloS One* 12 (7): e0180190.

Du, Juan, Jingjing Li, Jianhua Zhu, Chunhua Huang, Sixue Bi, Liyan Song, Xianjing Hu, and Rongmin Yu. 2018a. "Structural Characterization and

Immunomodulatory Activity of a Novel Polysaccharide from Ficus Carica." *Food & Function* 9 (7): 3930–43.

———. 2018b. "Structural Characterization and Immunomodulatory Activity of a Novel Polysaccharide from Ficus Carica." *Food & Function* 9 (7): 3930–43.

EFSA Panel on Dietetic Products, Nutrition and Allergies (NDA). 2010. "Scientific Opinion on the Substantiation of Health Claims Related to Pectins and Reduction of Post-prandial Glycaemic Responses (ID 786), Maintenance of Normal Blood Cholesterol Concentrations (ID 818) and Increase in Satiety Leading to a Reduction in Energy Intake (ID 4692) Pursuant to Article 13 (1) of Regulation (EC) No 1924/2006." *EFSA Journal* 8 (10): 1747.

Eliaz, Isaac, Arland T Hotchkiss, Marshall L Fishman, and Dorena Rode. 2006. "The Effect of Modified Citrus Pectin on Urinary Excretion of Toxic Elements." *Phytotherapy Research: An International Journal Devoted to Pharmacological and Toxicological Evaluation of Natural Product Derivatives* 20 (10): 859–64.

Espinal-Ruiz, Mauricio, Luz-Patricia Restrepo-Sánchez, Carlos-Eduardo Narváez-Cuenca, and David Julian McClements. 2016. "Impact of Pectin Properties on Lipid Digestion under Simulated Gastrointestinal Conditions: Comparison of Citrus and Banana Passion Fruit (Passiflora Tripartita Var. Mollissima) Pectins." *Food Hydrocolloids* 52: 329–42.

Gharibzahedi, Seyed Mohammad Taghi, Brennan Smith, and Ya Guo. 2019. "Ultrasound-Microwave Assisted Extraction of Pectin from Fig (Ficus Carica L.) Skin: Optimization, Characterization and Bioactivity." *Carbohydrate Polymers* 222: 114992.

Gunness, Purnima, and Michael John Gidley. 2010. "Mechanisms Underlying the Cholesterol-Lowering Properties of Soluble Dietary Fibre Polysaccharides." *Food & Function* 1 (2): 149–55.

Hasegawa, Yasushi, Yukiya Kadota, Chihiro Hasegawa, and Satoshi Kawaminami. 2015. "Lignosulfonic Acid-Induced Inhibition of Intestinal Glucose Absorption." *Journal of Nutritional Science and Vitaminology* 61 (6): 449–54.

Held, P. 2009. "An Absorbance-Based Cytotoxicity Assay Using High Absorptivity, Water-Soluble Tetrazolium Salts." *Application Note. BioTek Instruments, INC., Winooski, Vermont* 5404.

Jackson, Crystal L, Tina M Dreaden, Lisa K Theobald, Nhien M Tran, Tiffany L Beal, Manal Eid, Mu Yun Gao, Robert B Shirley, Mark T Stoffel, and M Vijay Kumar. 2007. "Pectin Induces Apoptosis in Human Prostate Cancer Cells: Correlation of Apoptotic Function with Pectin Structure." *Glycobiology* 17 (8): 805–19.

Lara-Espinoza, Claudia, Elizabeth Carvajal-Millán, René Balandrán-Quintana, Yolanda López-Franco, and Agustín Rascón-Chu. 2018. "Pectin and Pectin-Based Composite Materials: Beyond Food Texture." *Molecules* 23 (4): 942.

Lawaetz, O, A M Blackburn, S R Bloom, Y Aritas, and D N L Ralphs. 1983. “Effect of Pectin on Gastric Emptying and Gut Hormone Release in the Dumping Syndrome.” *Scandinavian Journal of Gastroenterology* 18 (3): 327–36.

Lea, Tor. 2015. “Caco-2 Cell Line.” *The Impact of Food Bioactives on Health*, 103–11.

Liu, Yanlong, Man Dong, Ziyu Yang, and Siyi Pan. 2016. “Anti-Diabetic Effect of Citrus Pectin in Diabetic Rats and Potential Mechanism via PI3K/Akt Signaling Pathway.” *International Journal of Biological Macromolecules* 89: 484–88.

Lobato-Calleros, C, J C Robles-Martinez, J F Caballero-Perez, E J Vernon-Carter, and E Aguirre-Mandujano. 2001. “Fat Replacers in Low-fat Mexican Manchego Cheese.” *Journal of Texture Studies* 32 (1): 1–14.

Lobato-Calleros, C, E J Vernon-Carter, J Sanchez-Garcia, and H S García-Galindo. 1999. “Textural Characteristics of Cheese Analogs Incorporating Fat Replacers.” *Journal of Texture Studies* 30 (5): 533–48.

Lorenzo, Carlo di, Cardiff M Williams, Ferenc Hajnal, and Jorge E Valenzuela. 1988. “Pectin Delays Gastric Emptying and Increases Satiety in Obese Subjects.” *Gastroenterology* 95 (5): 1211–15.

Makarova, Elina, Paweł Górnaś, Ilze Konrade, Dace Tirzite, Helena Cirule, Anita Gulbe, Iveta Pugajeva, Dalija Seglina, and Maija Dambrova. 2015. “Acute Anti-hyperglycaemic Effects of an Unripe Apple Preparation Containing Phlorizin in Healthy Volunteers: A Preliminary Study.” *Journal of the Science of Food and Agriculture* 95 (3): 560–68.

Martău, Gheorghe Adrian, Mihaela Mihai, and Dan Cristian Vodnar. 2019. “The Use of Chitosan, Alginate, and Pectin in the Biomedical and Food Sector—Biocompatibility, Bioadhesiveness, and Biodegradability.” *Polymers* 11 (11): 1837.

Min, Bockki, In Young Bae, Hyeon Gyu Lee, Sang-Ho Yoo, and Suyong Lee. 2010. “Utilization of Pectin-Enriched Materials from Apple Pomace as a Fat Replacer in a Model Food System.” *Bioresource Technology* 101 (14): 5414–18.

Naqash, Farah, F A Masoodi, Sajad Ahmad Rather, S M Wani, and Adil Gani. 2017a. “Emerging Concepts in the Nutraceutical and Functional Properties of Pectin—A Review.” *Carbohydrate Polymers* 168: 227–39.

———. 2017b. “Emerging Concepts in the Nutraceutical and Functional Properties of Pectin—A Review.” *Carbohydrate Polymers* 168: 227–39.

Nascimento, Georgia Erdmann do, Sheila Maria Brochado Winnischofer, Marcel Ivan Ramirez, Marcello Iacomini, and Lucimara Mach Côrtes Cordeiro. 2017. “The Influence of Sweet Pepper Pectin Structural Characteristics on Cytokine Secretion by THP-1 Macrophages.” *Food Research International* 102: 588–94.

Pappa, I C, J G Bloukas, and I S Arvanitoyannis. 2000. “Optimization of Salt, Olive Oil and Pectin Level for Low-Fat Frankfurters Produced by Replacing Pork Backfat with Olive Oil.” *Meat Science* 56 (1): 81–88.

Park, Jeongho, Qin Wang, Qi Wu, Yang Mao-Draayer, and Chang H Kim. 2019. "Bidirectional Regulatory Potentials of Short-Chain Fatty Acids and Their G-Protein-Coupled Receptors in Autoimmune Neuroinflammation." *Scientific Reports* 9 (1): 1–13.

Qi, Xin, Farage H Al-Ghazzewi, and Richard F Tester. 2018. "Dietary Fiber, Gastric Emptying, and Carbohydrate Digestion: A Mini-review." *Starch-Stärke* 70 (9–10): 1700346.

Schneeman, Barbara Olds, and Daniel Gallaher. 1985. "Effects of Dietary Fiber on Digestive Enzyme Activity and Bile Acids in the Small Intestine." *Proceedings of the Society for Experimental Biology and Medicine* 180 (3): 409–14.

Slavin, Joanne. 2013. "Fiber and Prebiotics: Mechanisms and Health Benefits." *Nutrients* 5 (4): 1417–35.

Slavin, Joanne L. 2008. "Position of the American Dietetic Association: Health Implications of Dietary Fiber." *Journal of the American Dietetic Association* 108 (10): 1716–31.

Sousa, RVRB, Maria Izabel Florindo Guedes, M M M Marques, D A Viana, I N G da Silva, P A S Rodrigues, and I G P Vieira. 2015. "Hypoglycemic Effect of New Pectin Isolated from Passiflora Glandulosa Cav in Alloxan Induced Diabetic Mice." *World Journal of Pharmacy and Pharmaceutical Sciences* 4 (1): 1571–86.

Taboada, Edelio, Patricio Fisher, Rory Jara, Elisa Zúñiga, Manuel Gidekel, Juan Carlos Cabrera, Eduardo Pereira, Ana Gutiérrez-Moraga, Reynaldo Villalonga, and Gustavo Cabrera. 2010. "Isolation and Characterisation of Pectic Substances from Murta (Ugni Molinae Turcz) Fruits." *Food Chemistry* 123 (3): 669–78.

Taboada, Edelio, Patricio Fisher, Rory Jara, Elisa Zuniga, Manuel Gidekel, Juan Carlos Cabrera, Eduardo Pereira, Ana Guti??rrez-Moraga, Reynaldo Villalonga, and Gustavo Cabrera. 2010. "Isolation and Characterisation of Pectic Substances from Murta (Ugni Molinae Turcz) Fruits." *Food Chemistry* 123 (3): 669–78. https://doi.org/10.1016/j.foodchem.2010.05.030.

Terpstra, A H M, J A Lapre, H T de Vries, and A C Beynen. 2002. "The Hypocholesterolemic Effect of Lemon Peels, Lemon Pectin, and the Waste Stream Material of Lemon Peels in Hybrid F1B Hamsters." *European Journal of Nutrition* 41 (1): 19–26.

Voragen, Alphons G J, Gerd-Jan Coenen, Rene P Verhoef, and Henk A Schols. 2009. "Pectin, a Versatile Polysaccharide Present in Plant Cell Walls." *Structural Chemistry* 20 (2): 263–75.

Wicker, Louise, Yookyung Kim, Mi-Ja Kim, Brittnee Thirkield, Zhuangsheng Lin, and Jiyoung Jung. 2014. "Pectin as a Bioactive Polysaccharide–Extracting Tailored Function from Less." *Food Hydrocolloids* 42: 251–59.

Zdunek, Artur, Piotr M Pieczywek, and Justyna Cybulska. 2021. "The Primary, Secondary, and Structures of Higher Levels of Pectin Polysaccharides." *Comprehensive Reviews in Food Science and Food Safety* 20 (1): 1101–17.

APPENDICES

APPENDIX A

2-DG6P STANDARD CURVE

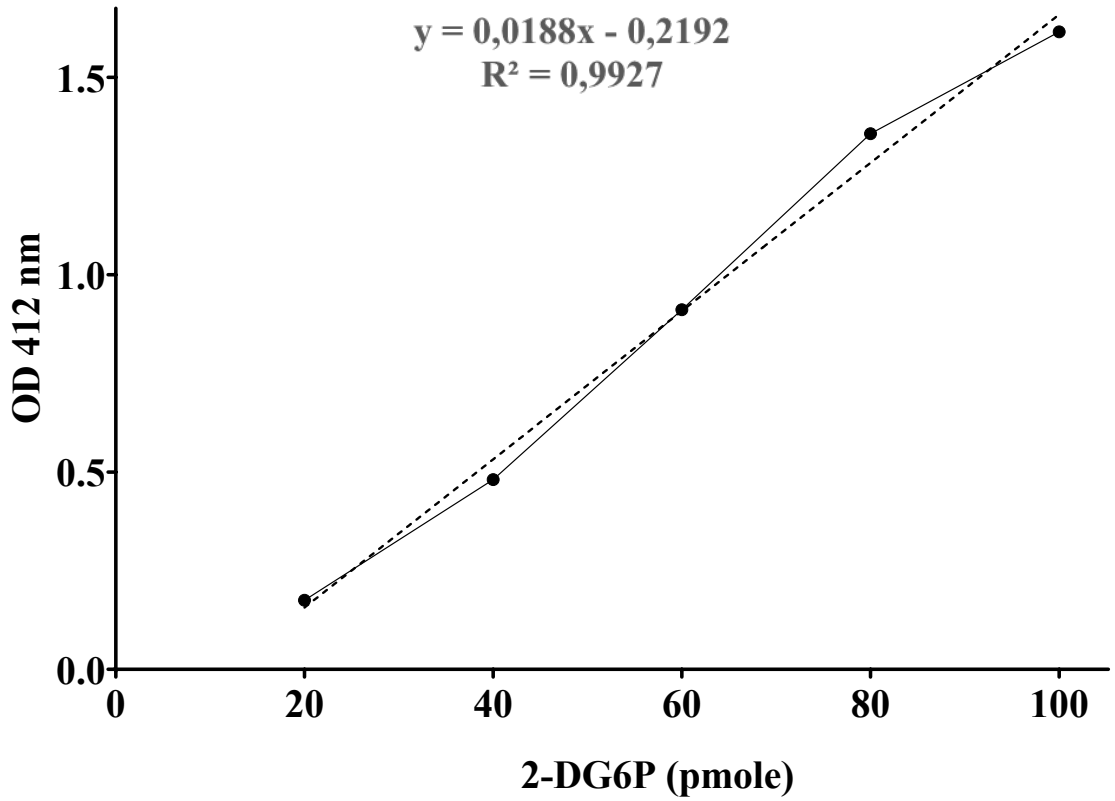

APPENDIX B

D-GLUCOSE STANDARD CURVE